ELSEVIER

Mobilization of arsenic and other naturally occurring contaminants in groundwater of the Main Ethiopian Rift aquifers

Tewodros Rango [a,*], Avner Vengosh [a], Gary Dwyer [a], Gianluca Bianchini [b]

[a] Division of Earth and Ocean Sciences, Box 90227, Nicholas School of the Environment, Duke University, Durham, NC 27708, United States
[b] Department of Physics and Earth Sciences, University of Ferrara, Via Saragat 1, 44100 Ferrara, Italy

ARTICLE INFO

ABSTRACT

This study investigates the mechanisms of arsenic (As) and other naturally occurring contaminants (F^-, U, V, B, and Mo) mobilization from Quaternary sedimentary aquifers of the Main Ethiopian Rift (MER) and their enrichment in the local groundwater. The study is based on systematic measurements of major and trace elements as well as stable oxygen and hydrogen isotopes in groundwater, coupled with geochemical and mineralogical analyses of the aquifer rocks. The Rift Valley aquifer is composed of rhyolitic volcanics and Quaternary lacustrine sediments. X-ray fluorescence (XRF) results revealed that MER rhyolites (ash, tuff, pumice and ignimbrite) and sediments contain on average 72 wt. % and 65 wt. % SiO_2, respectively. Petrographic studies of the rhyolites indicate predominance of volcanic glass, sanidine, pyroxene, Fe-oxides and plagioclase. The As content in the lacustrine sediments (mean = 6.6 mg/kg) was higher than that of the rhyolites (mean: 2.5 mg/kg). The lacustrine aquifers of the Ziway-Shala basin in the northern part of MER were identified as high As risk zones, where mean As concentration in groundwater was 22.4 ± 33.5 (range of 0.60—190 µg/L) and 54% of samples had As above the WHO drinking water guideline value of 10 µg/L. Field As speciation measurements showed that most of the groundwater samples contain predominantly (~80%) arsenate-As(V) over arsenite-As(III) species. The As speciation together with field data of redox potential (mean Eh = $+73 \pm 65$ mV) and dissolved-O_2 (6.6 ± 2.2 mg/L) suggest that the aquifer is predominantly oxidative. Water-rock interactions, including the dissolution of volcanic glass produces groundwater with near-neutral to alkaline pH (range 6.9—8.9), predominance of Na—HCO_3 ions, and high concentration of SiO_2 (mean: 85.8 ± 11.3 mg/L). The groundwater data show high positive correlation of As with Na, HCO_3, U, B, V, and Mo ($R^2 > 0.5$; $p < 0.001$). Chemical modeling of the groundwater indicates that Fe-oxides and oxyhydroxides minerals were saturated in the groundwater, suggesting that the As reactivity is controlled by adsorption/desorption processes with these minerals. The data show that As and other oxyanion-forming elements such as U, B, Mo, and V had typically higher concentrations at pH > ~8, reflecting the pH-dependence of their mobilization. Based on the geochemical and stable isotope variations we have established a conceptual model for the occurrence of naturally occurring contaminants in MER groundwater: 1) regional groundwater recharge from the Highland, along the Rift margins, followed by lateral flow and water—rock interactions with the aquifer rocks resulted in a gradual increase of the

salinity and naturally occurring contaminants towards the center of the valley; and (2) local $\delta^{18}O$-rich lake water recharge into adjacent shallow aquifers, followed by additional mobilization of As and other oxyanion-forming elements from the aquifer rocks. We posit that the combined physical-chemical conditions of the aquifers such as oxidizing state, Na−HCO$_3$ composition, and pH>∼8 lead to enhanced mobilization of oxyanion-forming elements from Fe-oxides and consequently contamination of local groundwater. These geochemical conditions characterize groundwater resources along the Eastern African Rift and thus constitute a potential threat to the quality of groundwater in larger areas of Eastern Africa.

1. Introduction

Elevated concentrations of arsenic (As) in groundwater have been reported in a wide range of geological environments (Smedley and Kinniburgh, 2002). This is important because consumption of high-As waters is known to have detrimental effects on human health (WHO, 2001; Chakraborti et al., 2002; Cheng et al., 2010; Yonus et al., 2011). Previous studies conducted in the USA (Robertson, 1989; Welch and Lico, 1998; Welch et al., 2000), China (Lianfang and Jianzhong, 1994; Guo et al., 2007), Chile (Borgono et al., 1977; Sancha and O'Ryan, 2008), Taiwan (Liu et al., 2006; Nath et al., 2008a,b, 2011; Reza et al., 2012; Lu et al., 2011; Li et al., 2011), West Bengal in India, and Bangladesh (Das et al., 1994; Mukherjee and Bhattacharya, 2001; Bhattacharya et al., 2002; Reza et al., 2010; Kar et al., 2010, 2011) have identified toxic levels of As in groundwater.

Dissolved As in groundwater can occur as either the reduced non-charged arsenite (As (III)) in the form of H_3AsO_3 species at pH below 9.2, or oxidized arsenate (e.g., $H_2AsO_4^-$ below pH ∼ 8.2) (Smedley and Kinniburgh, 2002). Numerous studies have shown that As in reduced environments tends to be mobilized into the liquid phase due to the predominance of non-charged arsenite (As (III)) (Smedley and Kinniburgh, 2002). The most common process that explains this mobilization is the reductive dissolution of iron and oxides/hydroxide minerals and subsequent release of As into the groundwater, which occurs under anaerobic conditions (Bhattacharya et al., 1997; Nickson et al., 2000; Dowling et al., 2002; Zheng et al., 2004; Mukherjee et al., 2008). Yet high As has also been found in oxidizing aquifers, such as the Caco-Pampean plain and loess aquifers in Argentina (Nicolli et al., 1989, 2010; Bundschuh et al., 2004; Gomez et al., 2009), northwestern and central Texas and the northern high plains of the USA (Nativ and Smith, 1987; Gosselin et al., 2006; Scanlon et al., 2009), and in the Taiyuan basin of northern China (Guo et al., 2007). In some of these oxidizing aquifers, other contaminants in the form of oxyanions such as V, B and Mo were also associated with elevated levels of As. One of the common geochemical features of these aquifers is the sodium-bicarbonate composition of the As-rich groundwater.

This study is focused in studying the mechanisms of As and other oxyanions mobilization from oxidizing aquifers in the Main Ethiopian Rift (MER). The MER is part of the East African Rift Valley system, and is characterized by extensive volcanic and tectonic activities that have led to formation of volcanic rocks and their weathered products, partially remobilized and redeposited as fluvio-lacustrine sediments (WoldeGabriel et al., 1990; Peccerillo et al., 2007).

Over 10 million inhabitants in the region depend primarily on groundwater for drinking and domestic purposes (Tekle-Haimanot et al., 1987; Kloos and Tekle-Haimanot, 1999). Yet elevated F$^-$ (Gizaw, 1996; Chernet et al., 2001; Rango et al., 2009) and As levels (Rango et al., 2010a, 2012) pose direct health risks to the local population (Reimann et al., 2003; Rango et al., 2012). The presence of naturally-occurring contaminants in the MER groundwater seems to directly link to geochemical processes that control the groundwater chemistry, in particular the interaction between the low saline groundwater that is discharged from the Rift escarpments with the aquifers rocks and sediments in the Rift valley floor.

The key geochemical process in MER that controls the groundwater chemistry is the silicate hydrolysis of the rhyolitic rocks that was initiated by high mantle CO_2 gas flux (Darling et al., 1996). The silicate hydrolysis generates dissolved sodium and bicarbonate together with solid weathering products (e.g., clay minerals and oxides) that enhance base−exchange reactions for removal of Ca^{2+} and Mg^{2+} and further release of Na^+. The end product is saline groundwater predominantly composed of a sodium-bicarbonate hydrochemical facies (Gizaw, 1996). In order to better understand the implications of the mentioned geochemical processes for water quality in the MER, this study carried out systematic analyses of field parameters (pH, temperature, electrical conductivity, redox potential) and sampling of various water sources from different parts of the MER, including groundwater, lakes, cold springs and geothermal springs (Fig. 1). Major and trace elements, As species distribution, and stable isotope composition were measured. In addition, this study evaluated the chemical and mineralogical compositions of the MER aquifer rocks (Quaternary lake sediments and volcanic rocks). We hypothesize that mobilization of trace elements such as As and B from the aquifer rocks is controlled by the chemical conditions of the groundwater. We use the water geochemistry combined with the stable isotopes of oxygen and hydrogen as proxies for evaluating the sources of the aquifer recharge water and to constrain the water−rock interactions (Clark and Fritz, 1997). Overall, we posit that understanding the geochemistry of As and other toxic elements and the mechanisms of their release into groundwater is important for deriving effective strategies for remediation of and/or minimizing exposures to contaminated aquifers. Furthermore, the findings from this study could have implications for neighboring regions in the
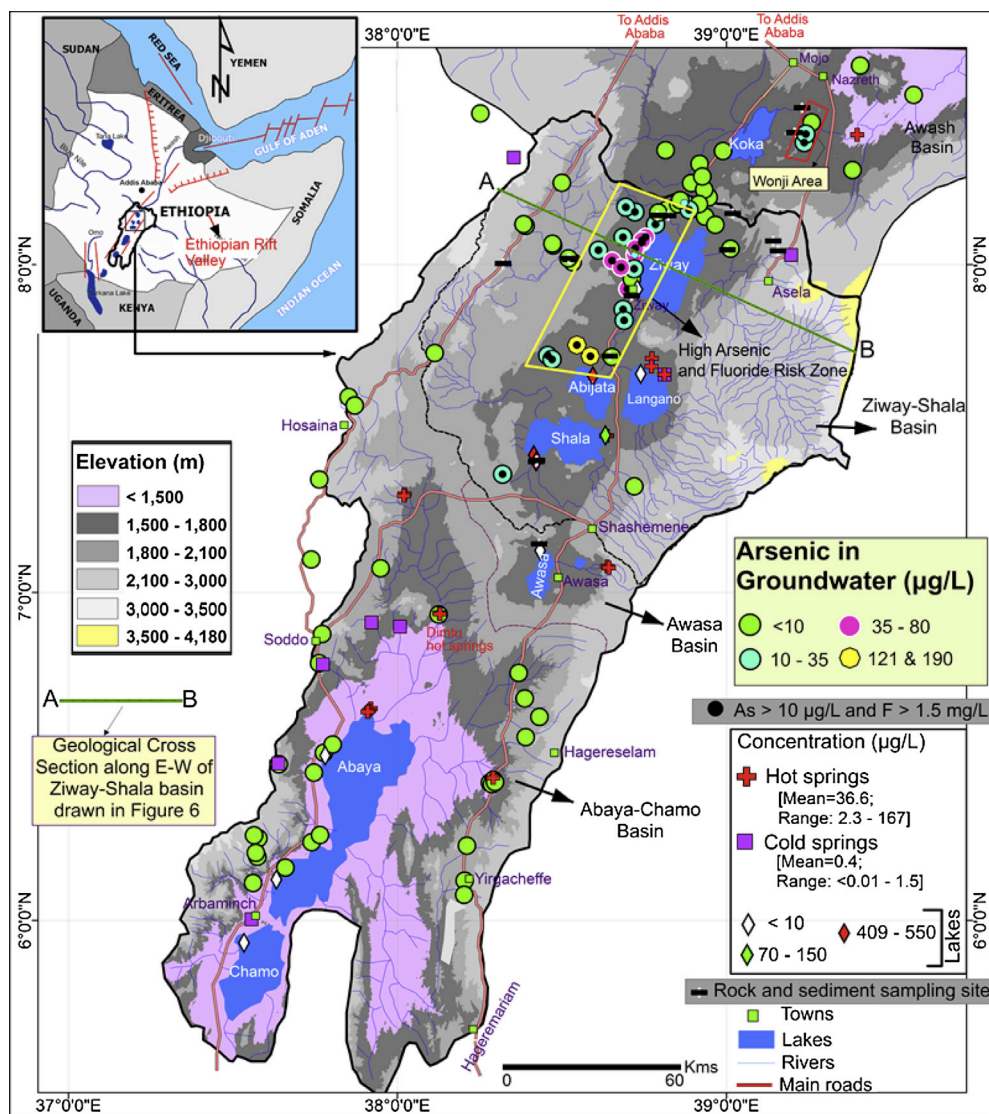
Fig. 1 – Distribution and identification of water sampling sites in this study according to type (groundwater, hot and cold springs, and lakes) and range of As levels. Groundwater concentrations are color-coded. Note that the yellow polygons represent zones with high As and black dots indicate wells with both high As and high fluoride (As > 10 μg/L and F > 1.5 mg/L).

East African Rift, showing analogous elevated levels of naturally occurring contaminants.

2. Materials and methods

2.1. Study area, geology and hydrogeology

The MER is characterized by a chain of lakes (Ziway–Langano–Abijata–Shala–Awasa-Abaya-Chamo) that lie at an average altitude of 1600 m above sea level (m.a.s.l). Within this region, the specific study area comprises two large basins, the Ziway-Shala and Abaya-Chamo basins, and a small catchment (Awasa) located in the central sector of the MER valley. These lakes receive surface inflow from rivers and springs that drain the western and eastern highlands (elevation above 2500 m.a.s.l. on average) bordering the MER.

The climate is humid to sub-humid in the highlands and escarpments and semi-arid to arid in the Rift valley, with aridity increasing towards the south. Mean annual rainfall in the highlands ranges from about 800 mm to over 2400 mm, while the Rift valley has rainfall varying from 300 mm to 800 mm (Ethiopian Mapping Authority, 1988). The mean annual temperature in the highlands is less than 15 °C and evaporation less than 1000 mm; on the Rift floor, mean temperature exceeds 20 °C and evaporation is more than 2500 mm (Le Turdu et al., 1999). Rainfall in the Rift primarily occurs in June to September, with additional modest rains in the period from March to May. During the long, dry period between October and February, surface water availability is low.

The surface geology of the Rift Valley region consists of volcanic deposits and sediments (Benvenuti et al., 2002). Most of the Rift floor is covered by silicic pyroclastic materials mainly consisting of rhyolitic ignimbrites, interlayered with basalts

and tuffs and associated with layered and unwelded pumices (Di Paola, 1972; Peccerillo et al., 2007). Lake Ziway plain, west of Lake Ziway is covered by lacustrine deposits of heterogeneous grain-size, including silt, clay, sand, and subordinate gravels. Due to the past influence of Rift's volcanic activity, the sediments contain a significant component of rhyolitic volcanic ash. The adjacent highlands, consists of basaltic lava flows, with inter-bedded ignimbritic horizons, overlaid by massive rhyolites, tuffs and basalts (Di Paola, 1972; WoldeGabriel et al., 1990). The topography slopes gently downward from the highlands towards Lake Ziway, where the volcanic products are covered by lacustrine sediments. Generally, the aquifers of the study area are represented by fractured volcanic rocks and ash-rich sediments. The presence of volcanic ash locally generates confined and semi-confined, with common depth to water table ranging from 20 to 80 m (Ayenew et al., 2008).

The Rift floor represents the regional discharge area, including perennial rivers, lakes and springs which outpour from tectonic structures of the escarpment (Ayenew et al., 2007). The floor of the Rift is also the site of geothermal circulation, and high temperature thermal springs emerge from the volcanic centres and active faults. Therefore, regional groundwater flow follows the topographic gradient from the highlands to the Rift floor across well-defined marginal faults forming escarpments and fractures in the Rift floor dotted by volcanic cones. Groundwater flow is controlled by a series of normal faults mainly oriented along the NE–SW Rift axis. Direct groundwater recharge takes place through fracture zones and then flow through alluvial/lacustrine deposits in river valleys. However, some of these faults locally act as groundwater barriers and form a series of swamps and seepage zones (Ayenew et al., 2008).

The groundwater chemistry of the region has been explored in detail in previous research (Darling et al., 1996; Gizaw, 1996; Ayenew, 1998; Chernet et al., 2001; Rango et al., 2009, 2010a; Bretzler et al., 2011; Furi et al., 2011). Two major hydrochemical facies have been identified: (1) low TDS; $Ca^{2+}(Mg^{2+})$–HCO_3^- water type that characterizes cold springs originating primarily from the basaltic highland outside the Rift; and (2) high TDS; Na^+–HCO_3^- water type that characterizes groundwater and geothermal waters emerging from the floor of the Rift. Most groundwater that originates from basaltic dominated aquifers outside the Rift is characterized by low salinity (generally EC < 400 μS/cm) with Ca^{2+} and Mg^{2+} as the dominant cation species. Groundwater from aquifers along the Rift escarpment as well as rapidly-recharged aquifers within the Rift floor maintain this $Ca^{2+}(Mg^{2+})$–HCO_3^- signature (Ayenew, 1998; Bretzler et al., 2011), and is also characterized by low levels of toxic elements such as F^- and As. In contrast, groundwater from the Rift floor is characterized by high-salinity and elevated concentrations of F^- and trace elements such as As and U (Reimann et al., 2003; Rango et al., 2012). Rango et al. (2012) has documented that 48 of the 50 (96%) wells in Ziway-Shala basin is characterized by F^- concentrations exceeding the guideline value of 1.5 mg/L for drinking water recommended by the World Health Organization (WHO). It was also shown that a large fraction of wells in the basin have concentrations of As (27 wells, 54%), U (11 wells, 22%), B (10 wells, 20%), and Mo (4 wells, 8%) exceeding the WHO drinking water guideline values of 10, 15, 500, and 70 μg/L, respectively.

Most of the previous research on groundwater in the MER has been focused on the geochemical evolution of sodium-bicarbonate groundwater and the processes that control F^- occurrence (Yirgu et al., 1999; Gizaw, 1996; Rango et al., 2009). It has been shown that the F^- content in groundwater is positively correlated with salinity, Na^+, and HCO_3^-, and inversely correlated with Ca^{2+} concentrations. Furthermore, solubility measurements indicate that low Ca^{2+} concentrations in the water limit the precipitation of F^- in the form of calcium fluoride (CaF_2); F^- therefore mobilizes readily and becomes a stable soluble species in Ca^{2+}-depleted groundwater.

2.2. Water sampling and analytical methods

Water samples were collected from 134 sources of various types over the course of two years (2010 and 2011) (94 groundwater wells, 8 cold springs, 21 geothermal springs, and 11 lakes; Fig. 1). The groundwater samples were collected from active pumping wells that were primarily used for drinking water. Water was allowed to flow for a few minutes from wells prior to sampling; samples from springs were collected at the mouth of the source, and lake samples were taken 50–100 m away from the lake shore.

In-situ measurements were conducted for pH, redox potential (Eh), dissolved O_2, temperature, and electrical conductivity (EC) using appropriate meters that were calibrated daily. Water samples were filtered in the field using 0.45 μm filters. Samples allocated for cation/trace metal analyses were filtered directly into 60 ml polyethylene bottles previously cleaned with pure ∼1N HCl and ∼1N HNO_3 and rinsed with deionized water having resistivity >18 MΩ*cm. The samples were immediately acidified with high-purity HNO_3 (Fisher Optima). Unfiltered and unacidified water samples were also collected into 60 ml and 30 ml polyethylene bottles respectively for measurement of alkalinity and hydrogen/oxygen isotopes.

Samples were also collected for As speciation analyses. Arsenic species were preserved in the field to eliminate changes that could be caused by metal (Fe, Mn) oxyhydroxide precipitation, photochemical oxidation, and redox reactions. Samples were filtered using 0.45 μm membrane syringe filter and poured through a solid-phase extraction cartridge (Supelco LC-SAX) with conditioning chloride form (2 ml of methanol; 10 ml of deionized water) and acetate form (10 ml of 1.7 M acetic acid; 10 ml of deionized water) to separate arsenite from arsenate. As (III) elutriate and As (V) plus other charged As species were extracted from LC-SAX cartridge with elution at an extraction flow rate of 1–2 drops per second. EDTA (ethylenediaminetetraacetic acid) preservatives were applied to minimize metal oxyhydroxide precipitation. This preservation technique was used on 59 water samples (52 groundwater wells, 7 hot springs).

Concentrations of major cations of calcium (Ca^{2+}), magnesium (Mg^{2+}), sodium (Na^+), and silica (SiO_2) were measured using a Fisons Spectraspan 7 direct-current plasma spectrometer (DCP) at Duke University calibrated using solutions prepared from single-element standards. Major anions of chloride (Cl^-), sulfate (SO_4^{2-}), and nitrate (NO_3^-) were analyzed using an ion chromatograph (IC). Fluoride content was determined by ion-selective electrode (ISE). Samples were mixed at a 1:1 volume ratio with a total ionic strength

adjustment buffer (TISAB) of pH 5–5.5, which allows optimal analyses of fluoride in the aqueous solution. Alkalinity (as HCO_3^-) was measured using titration techniques to pH 4.5. A wide spectrum of trace elements were analyzed via a VG Plasmaquad 3 inductively coupled plasma–mass spectrometer (ICP-MS) calibrated using serial dilutions of National Institute of Standards and Technology (NIST) 1643e standard spiked with U and Th in the analytical facilities at Duke University (USA).

Isotope ratios for hydrogen and oxygen in water were determined by a Thermofinnigan Delta + XL mass spectrometer at the Duke Environmental Isotope Laboratory. The isotopic ratios of $^2H/^1H$ and $^{18}O/^{16}O$ are expressed as δ notation $[\delta = 1000\,(R_{sample}/R_{standard} - 1)\%]$ with respect to the V-SMOW (Vienna Standard Mean Ocean Water) international standard.

The MINTEQV4 and WATEQ4F thermodynamic databases of the PHREEQC program (Parkhurst and Appelo, 1999) were used to simulate speciation of elements and calculate saturation indices (SI) in the groundwater samples.

2.3. Chemical and mineralogical analyses of the aquifer rocks

A total of 25 representative aquifer rocks (10 volcanic rocks and 15 sediments) were collected from outcrops in different locations of the study area, mostly from road and river cuttings. Polished thin sections were prepared from 8 selected samples and were investigated petrographically for mineral identification. Chemical analyses were carried out on all 25 solid samples using X-ray fluorescence spectrometry (XRF) on pressed powder pellets using wavelength-dispersive automated ARL Advant'X spectrometer at Ferrara University, Italy. Accuracy and precision, based on the replicate analyses of certified international standards, were estimated to be better than 3% for Si, Ti, Fe, Ca and K, 7% for Mg, Al, Mn, Na. Subsequently, 23 samples (10 sediments and 13 volcanic rocks) were selected for leaching experiments. In these experiments, powdered samples were mixed with double distilled water (pH = 4.6) at a ratio of 1:25 (1g/25 ml) at room temperature, and then shaken for 2 h at a frequency of 100 rev/min. These leaching experiments simulate the potential extractability (leachability) of soluble components during water–rock interactions. After separation from the residual solids, the effluents were filtered through 0.45 μm membrane filters. The analyses of As and other oxyanion-forming elements, as well as F^- on the leachates were carried out using ICPMS and IC, respectively.

For measurement of total As and other trace elements, 0.034 g of powdered rock and sediment samples were digested and analyzed by ICP-MS on a VG Plasmaquad 3 at Duke University following procedures described in Meurer et al. (1999). Reference materials used for instrument calibration and standardization included USGS certified geochemical reference materials DNC, G2, W2, BIR, SDO, SCO, SDC, AGV, and RGM and two in-house basaltic standards.

All digestion processes were prepared using ultra-pure HNO_3 and HF reagents (Fisher Optima) and double-distilled water (resistivity >18.2 MΩ*cm). All plastic polyethylene bottles and tubes were soaked with pure ~1N HCl and ~1N HNO_3, and then rinsed with deionized water.

3. Results and discussion

3.1. Physicochemical and elemental compositions of the MER waters

The pH of the groundwater samples from the floor of the MER ranged from near neutral to alkaline (range: 6.9–8.9). Temperature and Electric Conductivity (EC) varied from 25.8 to 40 °C (mean: 28 °C ± 3.7 °C) and 248 to 3970 μS/cm (mean: 1280 ± 767 μS/cm), respectively. High levels of Eh (most samples with Eh > +50 mV) were measured in groundwater wells (range: −146–229 mV; mean: +73 ± 65 mV). These analyses suggest that groundwater from the floor of the MER was under slightly to moderately oxidizing condition. The oxidizing condition of the MER groundwater is further confirmed by the presence of dissolved O_2, SO_4^{2-} and NO_3 and very low concentrations of other redox sensitive elements such as Fe and Mn. Among the sampled wells, only three samples originating from the Wonji area (Fig. 1) were characterized by more reducing conditions, recording lower Eh (−26, −130 and −146 mV).

Summary of selected element concentrations of the different water types is reported on Table 1. Most groundwater wells, geothermal waters, and lakes in the Rift had an exclusively Na^+–HCO_3^- composition and contained very low concentrations of Ca^{2+} and Mg^{2+}. Hot spring temperatures ranged from 38.6 to 93 °C, with a mean value of 67.14 ± 18.2 °C. Hot springs contained high concentrations of major and trace elements such as Na^+, HCO_3^-, F^-, As, B, U, V, Mo and SiO_2. The range of pH levels in the hot springs was similar to that in the groundwater wells. The mean Eh value of the hot springs was −71.5 ± 156, and most samples had dissolved O_2 below detection limit suggesting more anoxic conditions. Hot springs with relatively higher dissolved O_2 and positive Eh values were probably recharged by faster circulating groundwater from the highlands or nearby oxygenated lakes.

High SiO_2 concentrations (range: 56.8–111 mg/L; mean 85.8 ± 11.3) in the groundwater samples suggest an origin from the hydrolysis of silicate phases (including reactive volcanic glass) in the aquifer. This is demonstrated by calculating the (SI) of the mineral phases in the groundwater, using the PHREEQC hydro-geochemical model, which indicates saturation with important phases such as K-mica, kaolinite, Ca-montmorillonite, K-feldspar, albite, quartz, and chalcedony, consistent with the expected occurrence of silicate weathering products (see SI in Table 2). These results confirm earlier studies that suggest significant silicate weathering through silicate hydrolysis, which is the major process leading to the increased pH, Na^+ and HCO_3^- in the MER groundwater.

The lake waters were also dominated by Na^+ and HCO_3^- ions, with a wide salinity range from fresh (TDS ~400 mg/L in Lake Ziway) to saline water (TDS up to ~46,000 mg/L in Lake Chitu), and high alkalinity (pH as high as 10.14; Table 1). Other highly alkaline lakes were Shala and Abijata, with TDS of ~22,500 and ~41,000 mg/L, respectively. All of these lakes contain very low concentration of Ca^{2+} and Mg^{2+}. The low salinity of Lake Ziway is due to recharge of river water and frequent recycling of the water, whereas other Rift lakes are closed and are becoming saline by substantial evaporation.

Table 1 – Summary of pH, EC, Eh, DO and major and trace elements in waters sampled from groundwater wells, hot springs, cold springs, and lakes in the Ziway–Shala basin. Note: bd = below detection.

Parameters	Rift groundwater wells		Percentiles			Hot springs		Highland and escarpment (wells and cold springs)		Lakes	
	Min − max	Mean ± S.D	25th	50th	75th	Min − max	Mean ± S.D	Min − max	Mean ± S.D	Min − max	Mean ± S.D
pH	6.86–8.9	7.96 ± 0.5	7.69	8.0	8.14	6.78–8.4	7.58 ± 0.59	6.28–9.46	7.61 ± 1.0	6.87–10.1	8.77 ± 1.25
EC (μS/cm)	248–3969	1279 ± 77	766	1204	1689	775–22900	8847 ± 7851	88–873	384 ± 245	461–49480	19865 ± 20706
DO (mg/L)	3.52–14.5	6.6 ± 2.21	5.0	6.0	7.36	bd	bd	−92 −166	61.9 ± 73.7	−8–104	42.75 ± 46.46
Eh (mV)	−146–229	73.3 ± 65	40	77	113	−270 −163	−71.5 ± 156	15.4–31.7	24.0 ± 4.25	24.5–38.4	29.75 ± 4.50
Temp. (OC)	22.6–40.7	28.1 ± 3.7	26	27	30	38.6–93	67.14 ± 18.2	77–792	302 ± 205	400–45764	17290 ± 18367
Major ions (mg/L)											
F^-	1.06–61.6	9.21 ± 9.6	3.70	8.43	10.8	2.02–65	28.4 ± 25.6	0.2–3.0	1.17 ± 0.84	1.81–316	116 ± 118
Cl^-	2.25–252	48.3 ± 56.8	9.88	24.1	64.7	30.8–1634	697 ± 651	1.39–19.0	8.71 ± 6.50	15.9–5839	2330 ± 2506
NO_3^-	bd − 21.2	1.55 ± 3.6	0.21	0.47	1.35	0.26–6.04	2.05 ± 1.70	0.01–1.40	0.53 ± 0.45	−0.22 −11.3	3.35 ± 3.82
SO_4^{2-}	bd − 475	30.5 ± 70.4	3.06	7.81	26.5	2.23–255	82.24 ± 88.4	1.15–13.7	6.29 ± 4.38	4.15–701	232 ± 252
HCO_3^-	162–2045	667 ± 369	428	612	894	283–3455	1667 ± 1205	54.0–564	208 ± 144	267–30376	10819 ± 11881
Ca^{2+}	0.93–90	16.8 ± 16.9	5.39	12.8	20.3	1.15–21.52	6.76 ± 7.24	1.19–65	26.5 ± 24.7	2.81–14.4	7.25 ± 3.79
Mg^{2+}	0.07–38	4.85 ± 6.1	1.28	3.43	5.98	0.08–16.5	4.04 ± 6.04	0.10–17.5	7.02 ± 5.90	0.39–8.63	2.67 ± 3.11
Na^+	34.8–1111	277 ± 200	145	240	378	105–2483	1160 ± 921	4.0–166	48.7 ± 43.2	82.3–9034	3773 ± 3745
SiO_2	56.8–111	85.8 ± 11.3	78.9	85.8	93.4	84.3–214	125 ± 43.9	bd − 89.0	59.8 ± 30.0	37.5–227	108 ± 62.3
Trace elements (μg/L)											
As	0.60–190	22.4 ± 33.5	4.19	11.1	21.9	3.79–167	61.8 ± 63	0.25–1.96	0.89 ± 0.50	2.39–566	165 ± 215
U	0.06–69.0	10.4 ± 14.3	1.98	4.74	10.3	0.003–8.69	1.4 ± 2.73	bd − 15.4	3.36 ± 5.20	0.47–121	42.6 ± 42.6
B	14.8–2100	310 ± 353	88.6	228	415	241–8646	3936 ± 3313	3.56–82.8	18.2 ± 21.6	87.3–30972	11402 ± 11752
V	0.42–150	28.0 ± 35.8	2.74	18.9	37.5	2.09–22.62	9.17 ± 6.57	0.76–26.6	10.1 ± 6.90	2.14–110	52.3 ± 41.9
Mo	1.53–128	24.3 ± 30.2	6.83	10.7	27.6	23.74–452	123 ± 125	0.02–14.0	2.82 ± 3.80	4.3–7713	1428 ± 1600
Se	Bd −18.4	2.01 ± 2.90	0.55	1.17	2.43	0.95–37.3	16.5 ± 13.7	0.09–7.20	1.37 ± 1.90	0.7–96.7	39.2 ± 40.8
Cr	0.06–14.2	2.21 ± 2.81	0.58	1.15	2.59	0.96–38.1	17.2 ± 14.0	0.23–4.20	1.43 ± 1.17	1.36–83	36.9 ± 35.0
Fe	bd − 472	61.4 ± 88.0	13.8	41.4	58.8	6.83–763	227 ± 244	15.9–1251	216 ± 350	42.9–1966	609 ± 627
Al	1–131	12.5 ± 23.8	4.59	6.78	10.6	5.35–733	153 ± 234	5.68–2181	444 ± 817	22.8–8700	1253 ± 3032
Mn	0.02–748	68 ± 185	0.50	2.97	14.8	0.28–202	31.6 ± 60.7	0.65–408	45.7 ± 115	5.17–97.0	25.9 ± 29.4
Co	0.004–0.30	0.07 ± 0.06	0.03	0.05	0.09	0.004–0.32	0.10 ± 0.11	bd − 0.34	0.11 ± 0.1	0.08–1.93	0.97 ± 0.63
Cd	0.002–0.30	0.04 ± 0.05	0.01	0.03	0.04	0.04–0.85	0.39 ± 0.31	bd − 1.25	0.12 ± 0.36	0.011–8.10	1.90 ± 2.75
Ni	0.01–5.70	0.48 ± 0.81	0.18	0.30	5.70	0.16–2.56	1.18 ± 0.88	0.08–4.06	0.95 ± 1.08	0.31–12.0	5.64 ± 3.84
Sb	0.002–1.3	0.23 ± 0.27	0.45	0.12	0.33	bd − 6.40	2.05 ± 2.50	bd − 6.30	0.56 ± 1.81	0.07–4.37	1.23 ± 1.52
Cu	0.13–29.3	3.05 ± 5.70	0.38	0.78	2.71	0.04–1.76	0.65 ± 0.56	0.13–5.74	1.58 ± 1.6	0.53–7.11	3.87 ± 2.19
Zn	bd − 355	51.0 ± 66.3	13.9	27.6	62.3	bd − 1.90	0.19 ± 0.60	bd − 299	84.9 ± 101	bd − 18.4	2.93 ± 6.40
Ag	bd − 0.10	0.015 ± 0.02	bd	0.01	0.02	0.002–0.14	0.06 ± 0.05	bd − 0.11	0.04 ± 0.04	0.034–0.46	0.24 ± 0.17
Sr	2.2–717	123 ± 123	43.6	90.3	154	30.8–459	215 ± 134	3.2–297	120 ± 105	50–187	102 ± 47.0
Be	0.01–1.10	0.14 ± 0.20	0.06	0.09	0.12	0.04–20.1	5.6 ± 7.63	bd − 0.53	0.10 ± 0.14	0.12–2.78	1.23 ± 1.10
Li	4.94–105	49 ± 24.5	31.2	43.4	70.0	10.9–659	394 ± 278	0.87–15.7	6.9 ± 5.02	2.83–113	47.0 ± 46.0
Rb	3.14–61.6	15.2 ± 11.2	9.64	11.8	15.8	26.4–205	127 ± 73.0	0.82–52.6	13.6 ± 13.4	7.7–1180	233 ± 391
Br	0.04–1.55	0.42 ± 0.35	0.18	0.31	0.58	0.21–6.90	2.60 ± 2.85	0.05–0.27	0.11 ± 0.07	0.17–28.1	9.03 ± 9.9
Ba	0.41–131	12.8 ± 26.0	1.44	3.75	12.4	0.22–60.4	23.4 ± 20.7	0.01–38.4	9.71 ± 10.1	7.3–41.0	26.1 ± 10.1
Pb	bd − 3.70	0.52 ± 0.82	0.08	0.19	0.47	0.01–0.67	0.22 ± 0.23	bd − 1.95	0.45 ± 0.63	0.06–3.40	1.30 ± 1.22

Table 2 – Equilibrium molalities of the main aqueous species of As, U, B and V and speciation simulation indicates that As(V), U(VI), B(OH)$_3$ and V(V) are the thermodynamically stable species in oxidizing conditions.

Species	Molality	As, U, B and V species				Phases	SI
Na^+	1.96E-02	Arsenic				Albite ($NaAlSi_3O_8$)	0.98
K^+	2.56E-04	As(V)	7.369e-07	U (VI)	1.075e-07		
Ca^{2+}	1.54E-04	$HAsO_4^{-2}$	7.159e-07	$UO_2(CO_3)_3$-4	1.054e-07	Calcite ($CaCO_3$)	0.48
Mg^{2+}	1.72E-04	$H_2AsO_4^-$	1.988e-08	$UO_2(CO_3)_2$-2	2.050e-09		
F^-	9.07E-04	As(III)	3.741e-16	U (V)	4.555e-18	Dolomite ($CaMg(CO_3)_2$)	1.20
$Cl-$	8.67E-04	H_3AsO_3	3.319e-16	UO_{2+}	4.555e-18	Fluorite (CaF_2)	0.07
SO_4^{2-}	7.92E-05	$H_2ASO_3^-$	4.224e-17	U (IV)	2.099e-18	Goethite (FeOOH)	5.67
NO_3^-	3.22E-05			U ($OH)_5^-$	2.099e-18	Hematite (Fe_2O_3)	13.7
HCO_3^-	1.93E-02					Gibbsite ($Al(OH)_3$)	−0.50
Fe	7.49E-07					Chalcedony (SiO_2)	0.71
Mn	2.10E-08					Quartz (SiO_2)	1.16
Al	3.26E-07	Boron		Vanadium		K-feldspar ($KAlSi_3O_8$)	2.09
Si	1.57E-03	B	6.022e-05	V(V)	8.416e-07	Illite ($K_{0.6}Mg_{0.25}Al_{2.3}Si_{3.5}O_{10}(OH)_2$)	1.64
As	7.37E-07	H_3BO_3	5.276e-05	$H_2VO_4^-$	4.626e-07	Kaolinite ($Al_2Si_2O_5(OH)_4$)	2.10
B	6.02E-05	$H_2BO_3^-$	7.232e-06	HVO_4-2	3.787e-07	K-mica ($KAl_3Si_3O_{10}(OH)_2$)	3.27
V	8.45E-07					Ca-montmorillonite ($Ca_{0.16}5Al_{2.33}Si_{3.67}O_{10}(OH)_2$)	1.60
U	1.08E-07					Talc ($Mg_3Si_4O_{10}(OH)_2$)	5.00

Speciation and saturation indices derived from PHREEQC geochemical code for an oxidizing groundwater well Mean field parameters: ($T = 26.9$ °C; pH: 8.29; Eh: 113).

3.2. Arsenic and other oxyanion-forming elements in MER groundwater and their speciation

The spatial distribution of As concentrations in the different water sources is shown in Fig. 1. In the Ziway-Shala basin, As in the groundwater ranged from 0.6 to 190 µg/L, with a mean of 22.4 ± 33.5 µg/L; 20% of samples contained As concentrations >30 µg/L. The areas near lakes Ziway and Koka are indicated by the polygons (see Fig. 1) and represent zones with consistently high As concentrations (As >10 µg/L) in groundwater. These zones also overlap with high F^- areas (F^- >1.5 mg/L). Arsenic levels were much lower in the southern basins (e.g. Abaya-Chamo, mean: 0.7 ± 1.1 µg/L) of the Rift Valley.

Field based As speciation measurements revealed that As in nearly 95% of the groundwater samples is composed of predominantly (over 80%) arsenate −As(V) rather than arsenite −As(III) species, confirming the oxidizing condition of the groundwater. In contrast, As occurred mainly as As(III) in the hot springs, suggesting more reducing conditions. Excluding the samples taken from three reducing groundwater wells, all MER groundwater samples had As(V)/As$_{Total}$ ratios of 0.56−0.98 (42 wells). These results are consistent with the field measurements of high dissolved O_2 and Eh, which confirms that most of the MER groundwater is under oxidizing condition. Similarly, PHREEQC speciation modeling revealed that As(V) species in the groundwater samples are predominantly $HAsO_4^{2-}$ and $H_2AsO_4^-$.

Significant variations in the concentrations of other metals were found in the MER groundwater (Table 1). *Uranium* concentrations varied between 0.6 and 68.6 µg/L with a mean of 9.2 ± 9.6 µg/L. The dominant dissolved species in the oxidized groundwater were uranyl carbonate complexes ($UO_2CO_3^{2-}$; $UO_2CO_3^{4-}$). In contrast, uranium concentrations in the three groundwater wells under more reducing conditions were significantly lower, possibly due to immobilization by

reduction to U(IV), with subsequent precipitation under anaerobic conditions (e.g., Smedley et al., 2003).

Vanadium concentrations varied between 0.4 and 150 µg/L with a mean of 28 ± 35.8 µg/L. In the oxidizing groundwater vanadium occurred predominantly as vanadate (HVO_4^{2-}; $H_2VO_4^-$) species. *Molybdenum*, which occurred primarily as hexavalent Mo(VI) and (MoO_4^{2-}) forms, ranged in concentrations from 1.5 to 128 µg/L, with a mean of 24.3 ± 30.17 µg/L. *Selenium* concentrations ranged from below detection limit to 18.4 µg/L (mean: 2.0 ± 2.9 µg/L). The sample with the highest Se (18.4 µg/L) was found in a lacustrine sediment aquifer. Selenium mostly occurred as $HSeO_3^-$ and SeO_3^{2-} species. *Boron* concentrations varied from 14.8 to 2100 µg/L with a mean of 310 ± 353 µg/L. Boron was composed of $B(OH)_3$ and/or $B(OH)_4^-$ species.

Chromium concentrations ranged from 0.06 to 14.2 µg/L with a mean of 2.2 ± 2.8 µg/L. Despite its preferential mobility under oxidizing conditions, Cr concentrations are generally low in these samples. This is likely due to the low concentration of Cr in MER rhyolitic igneous rocks (Table 3). *Antimony* concentrations varied from 0.002 to 1.3 µg/L (mean: 0.23 ± 0.27 µg/L). This range is below the permissible limit WHO guideline value of 20 µg/L (WHO, 2006).

3.3. Other trace elements distribution in the MER groundwater

Concentrations of toxic transition metals (such as Ni^{2+}, Co^{2+}, Cd^{2+}, Cu^{2+}, Zn^{2+}, Pb^{2+} and Ag^{2+}) were generally low in the MER groundwater samples (Table 1). Nickel had a mean concentration of 0.48 ± 0.81 µg/L (maximum of 5.6 µg/L), which is well below the drinking water guideline threshold (70 µg/L). The maximum concentrations of Cu and Zn were 29.3 (mean: 3.1 ± 5.7 µg/L) and 355 µg/L (mean: 51 ± 66 µg/L), respectively. Cu content was below the WHO guideline value

Table 3 – Statistical summary (minimum, maximum, mean and SD (standard deviation) of a) XRF analyses result displaying major ion oxides b) Total content of trace elements from complete acid digestion and c) Water extractable oxyanion-forming trace elements (including fluoride) on MER rock (ignimbrites, tuff, pumice and obsidians (n = 13) and lacustrine sediments (n = 7), fluvial sediments (n = 2), and a basalt sample. bd- below detection.

	Min.	Max.	Mean	SD	Min.	Max.	Mean	SD	Min.	Max.	Mean	SD	
	Rhyolites (n = 10)				Lacustrine sediments (n = 3)				Fluvial sediments (n = 2)				Basalt (n = 1)
a) Oxides (wt.%)													
SiO_2	67.7	75.8	72.1	2.4	49.7	67.6	60.6	9.63	70.3	71.8	71.1	1.03	50.6
TiO_2	0.27	0.68	0.47	0.15	0.33	0.64	0.48	0.15	0.36	0.37	0.37	0.01	2.49
Al_2O3	9.32	12.0	10.2	0.86	1.76	9.55	6.51	4.17	8.52	8.75	8.64	0.16	16.7
Fe_2O_3	4.62	7.33	5.69	0.75	1.01	5.29	3.80	2.42	6.66	8.05	7.36	0.98	12.1
MnO	0.11	0.34	0.21	0.06	0.06	0.22	0.15	0.09	0.23	0.24	0.23	0.01	0.17
MgO	0.01	1.33	0.39	0.41	1.36	24.7	9.97	12.8	0.12	0.41	0.26	0.20	3.44
CaO	0.19	0.99	0.54	0.31	3.36	4.53	4.02	0.60	0.24	0.29	0.26	0.04	9.05
Na_2O	0.97	5.63	4.07	1.30	1.88	3.81	2.74	0.98	2.87	3.88	3.38	0.71	3.70
K_2O	2.31	4.45	4.02	0.61	0.62	3.12	2.11	1.31	4.28	4.68	4.48	0.28	1.33
P_2O_5	bd	0.16	0.04	0.06	0.05	0.08	0.07	0.02	bd	bd	bd	bd	0.41
LOI	bd	5.67	2.00	1.85	5.58	14.7	9.50	4.67	3.29	4.64	3.97	0.95	bd
b) Trace elements (mg/kg)													
As	1.13	3.50	2.46	0.63	1.42	16.1	6.62	5.99	2.34	3.02	2.68	0.49	0.59
U	1.73	6.72	3.64	1.31	2.18	12.2	4.37	3.52	4.06	4.46	4.26	0.28	0.68
V	2.96	28.0	10.9	8.35	21.0	199	62.3	61.7	4.71	5.90	5.30	0.84	334.7
Mo	0.93	8.69	4.58	1.92	2.29	904	136	338	5.33	5.50	5.41	0.12	1.07
Cr	0.90	21.7	4.82	5.39	8.86	27.2	15.9	6.72	1.73	3.46	2.60	1.22	40.3
Sc	0.43	11.34	3.05	2.85	2.76	6.95	4.64	1.48	0.99	1.39	1.19	0.28	28.4
Rb	82	129	108	15.9	28.1	102	75.0	24.3	119	125	122	4.33	25.8
Zr	799	1557	957	195	127	793	564	227	973	1015	994	30.14	196
Ce	172	387	219	53.0	35.2	200	142	57.9	225	233	229	5.35	58.9
La	89.3	171	108	22.8	16.1	96.1	68.9	29.3	109	114	111	3.53	27.3
Nb	116	225	138	28.8	20.5	135	89.3	36.8	148	152	150	2.93	32.0
Y	77.1	187	108	28.3	17.4	97.1	67.3	28.8	109	118	113	6.71	31.0
Ba	16.8	796	217	259	66.4	285	181	79.6	18.4	27.7	23.1	6.58	389
Ni	0.00	12.00	1.99	3.25	6.33	18.6	10.1	4.39	0.01	0.77	0.39	0.54	25.4
Co	0.12	5.73	1.30	1.53	2.66	5.63	4.52	1.30	0.30	0.57	0.43	0.19	40.2
Sc	0.43	11.3	3.05	2.85	28.4	2.76	6.95	4.64	1.48	0.99	1.39	1.19	0.28
Cu	1.57	11.7	4.11	2.72	4.40	11.30	7.19	2.19	2.06	2.42	2.24	0.26	64.4
Zn	159	328	216	42.2	115	45.8	181	127	44.5	207	218	213	7.61
Pb	12.9	24.4	18.5	3.80	4.38	2.51	14.2	10.3	3.77	18.66	20.33	19.49	1.18
Be	5.58	9.59	6.60	1.03	1.32	0.80	6.24	4.60	1.84	6.79	7.30	7.05	0.36
Sr	1.07	87.7	22.9	24.4	499	71.3	775	344	266	4.60	5.71	5.16	0.78
Li	6.76	39.2	26.7	9.72	7.58	32.4	132	78.8	39.7	25.9	29.9	27.9	2.82
c) Water soluble components (mg/kg)													
As	bd	0.02	0.01	0.01	0.003	6.74	1.71	2.58	bd	0.04	0.02	0.03	0.01
U	bd	0.01	0.001	0.003	0.001	1.09	0.20	0.40	bd	0.003	0.003	bd	0.001
Mo	bd	1.34	0.18	0.41	bd	819	123	307	0.02	0.03	0.03	0.00	0.16
V	bd	0.26	0.08	0.08	0.04	51.4	9.30	18.9	0.02	0.14	0.08	0.09	0.06
B	bd	0.58	0.10	0.16	0.22	27.0	7.87	10.4	0.06	0.20	0.13	0.10	0.07
Se	bd	0.01	0.003	0.004	bd	1.09	0.21	0.40	bd	0.003	0.002	0.002	0.01
F	2.59	63.8	17.4	17.0	5.88	241	93.5	96.1	6.86	8.20	7.53	0.95	3.89

(2000 µg/L). In contrast, Zn concentrations were higher, compared to other transition metals, perhaps due to the higher concentration in the rhyolites (Table 3). No guideline value exists for Zn as it typically occurs in natural surface waters at concentrations below 10 µg/L, and in groundwater between 10 and 40 µg/L (Elinder, 1986). Lead concentrations were lower than 3.7 µg/L, which is below the guideline value (10 µg/L). Barium concentrations were also relatively low, ranging from 0.41 to 131 µg/L with a mean of 12.8 ± 26 µg/L. All the groundwater wells are well below the drinking water guideline value (0.7 mg/L) for drinking water. The concentrations of other metals (Co, Cd, Ag, Sr, Be, Li, Rb, and Pb) are reported in Table 1.

Unlike oxyanion-forming elements, most transition metals become increasingly insoluble with increasing pH. Their solubility is strongly limited by precipitation, or coprecipitation, with oxides, hydroxides, carbonate or phosphate minerals, or more likely by their strong adsorption to hydrous metal oxides, clay, and organic matter (Smedley and Kinniburgh, 2002). These processes are consistent with the observed inverse relationship in MER groundwater between As concentration and Fe, Mn, Al, Ba, Cu, Pb, Zn, and Ni concentrations.

3.4. Relationship between arsenic and other water quality parameters in groundwater

Elevated concentrations of As (and other oxyanion-forming elements) were generally found at near neutral to high pH, with the highest levels found in waters at pH ranging between ~8.1 and 8.9 (Fig. 2a; shaded block). Similarly, high concentrations of F^-, B, Mo, U, Se, Sb, and Cr (Figure not shown) were found in waters of pH above ~8. Arsenic concentrations were positively correlated with Na^+, alkalinity (as HCO_3^-), B, U, V, Mo, and Sb ($r > 0.5$; $p < 0.001$). Weak to moderate correlations were also observed between As and F^-, Cl^-, Se, and Cr ($r < 0.5$; $p < 0.05$). There is no clear linear correlation between As and Eh, but elevated As and V were found only in groundwater of positive Eh values (range: 10—150 mV; Fig. 2b; shaded block).

The concentrations of dissolved Fe and Mn in the groundwater samples varied from <0.01 to 472 µg/L and from 0.02 to 748 µg/L respectively. The highest Fe concentrations were found in reducing groundwaters (389 and 472 µg/L) and in the samples characterized by near neutral pH. Since these groundwater samples are under anoxic conditions, Fe^{2+} persists in these waters at relatively higher concentration. Likewise, high Mn (671 and 748 µg/L) levels occurred in the reducing waters.

The variations of Fe and Mn in this system could explain the As mobility due to the closed geochemical association between Fe, Mn and As, and the ability of Fe-oxyhydroxides to adsorb As (Smedley and Kinniburgh, 2002). Under oxidizing conditions, the solubility of Fe and Mn oxyhydroxides is low and therefore concentration of dissolved Fe and Mn were also low in the MER groundwater. High concentrations of Fe were found only in waters with pH between 7.2 and 7.8. The highest concentrations of Fe and Mn in the MER groundwater were found at pH of 7.3, and these concentrations generally decrease with increasing pH. It has been shown that dissolved Fe in groundwater is directly controlled by the pH due to the dependence of oxidation/precipitation equilibrium to the acidity level of the water (Stumm and Morgan, 1996).

Speciation of As and the stability of As controlling solid phases were also determined using the PHREEQC geochemical modeling program (Parkhurst and Appelo, 1999). The mineral saturation index was calculated with respect to most of the Fe-, Al-, and Mn-bearing oxyhydroxides, as well as clay minerals. The results of this analysis show that the oxidizing and reducing groundwater are predominantly saturated with respect to Fe-oxides and -oxyhydroxides, and clay minerals such as K-mica, kaolinite, Ca-montmorillonite, Illite, K-mica, and chlorite, suggesting these phases are likely to precipitate as shown in the reaction below:

$$2Fe^{2+} + 1/2O_2 + 3H_2O = 2FeOOH + 4H^+$$
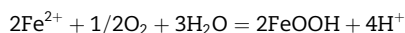
Due to the high adsorption capacity of Fe-oxides and -oxyhydroxides and clay minerals, these mineral phases have the capacity to control the reactivity and thus the concentrations of As and other oxyanion elements in the aquifer (Smedley and Kinniburgh, 2002). The Fe phases are plausibly responsible for the poor correlation between As and Fe (Fig. 3). Arsenic-bearing phases were undersaturated in the groundwater and thus had only limited influence on As mobilization.
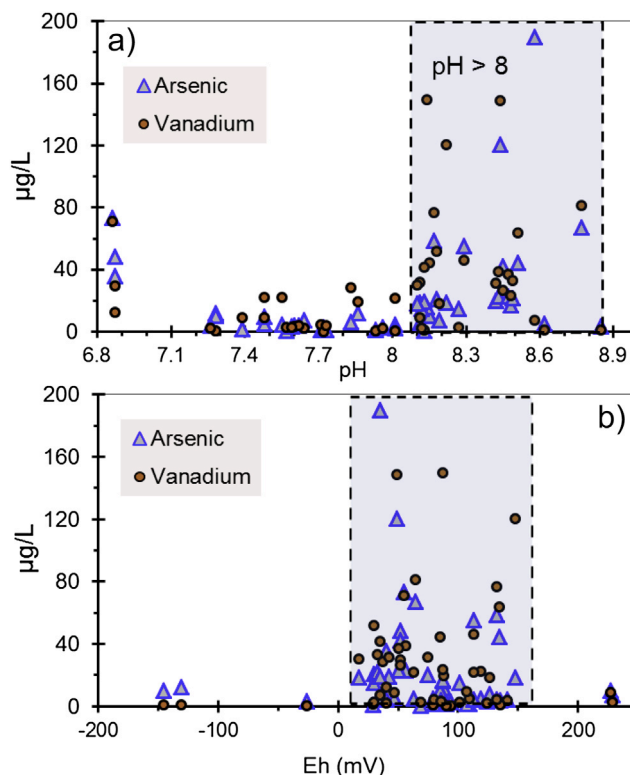

Fig. 2 — a) Plots of total As and V with pH and b) total As and V with Eh in groundwater samples. Note that at pH < 8, the average As concentration is close to 11 µg/L, whereas 33 µg/L at pH > 8.

We conclude that As concentrations in the MER groundwater were principally governed by adsorption—desorption reactions with Fe oxyhydroxides.

3.5. Mineralogical and geochemical compositions of the MER aquifer rocks

Petrographic investigation of rhyolites and lacustrine sediments showed that they contained on average 60% volcanic glass, 8.25% sanidine, 4.8% pyroxene, 3% plagioclase, 3.8% iron
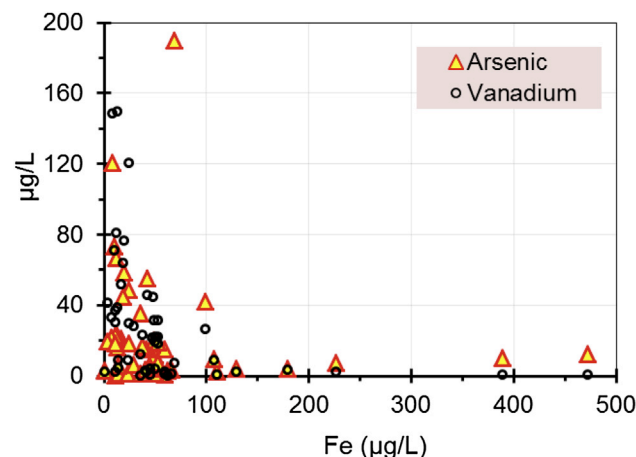

Fig. 3 — Inverse relationships between Fe with As and V.

oxides, as well as minor occurrences of biotite and quartz. Calcite was also found in the lacustrine sediments. Potential As-bearing phases were not found in this thin-section investigation. Table 3a displays the chemical composition of major oxides in rocks and sediments as determined by the XRF analysis. The compositions of ignimbrite, pumice, tuff, and obsidian are typically rhyolitic with high average concentrations of SiO_2 (∼68 wt%), Fe_2O_3 (5.7 wt%), Al_2O_3 (10.2 wt%), Na_2O (4.07 wt%), and K_2O (4.02 wt%). Moreover, the rhyolites were rich in incompatible elements like Rb (107.6 mg/kg), Zr (957 mg/kg), Ce (219 mg/kg), La (108 mg/kg), Nb (116 mg/kg), and Y (108 mg/kg), and were depleted in compatible elements like Ni (2 mg/kg), Cr (4.8 mg/kg), Co (1.3 mg/kg), and Sc (3 mg/kg) (Table 3b).

Total SiO_2 and Fe_2O_3 contents in sediments ranged from 49.7–72.4 wt.% and 1.0–8.1 wt.% respectively. The high content of silica in these materials suggests that aquifer materials contain significant amounts of volcanic glass of rhyolitic composition.

3.6. Sources and mobilization of arsenic

Total contents of As and other trace elements including U, V, Mo, and Cr in volcanic rocks and sediments from MER are reported in Table 3b. Arsenic ranges in rhyolites and sediments were 1.1–3.5 mg/kg (mean: 2.5 mg/kg) and 1.4–16.1 mg/kg (mean: 6.6 mg/kg), respectively. These values are not very different from average As values found in similar sediments reported elsewhere, which typically range of 5–10 mg/kg (Webster, 1999; Smedley and Kinniburgh, 2002). The samples with the highest As concentrations of 16.1, 9.7 and 12.2 mg/kg were found in lacustrine sediments; all other analyzed rocks and sediments had lower As contents in the range of 0.6–3.5 mg/kg. Not unexpectedly, the lowest As (0.6 mg/kg) was measured on basalt. The lacustrine sediments also contained on average 3.5 mg/kg of U, 62 mg/kg of V, 136 mg/kg of Mo, and 6.7 mg/kg of Cr, which are much higher than the respective concentrations measured in rhyolites.

Other studies in similar geological settings have found that As concentrations in volcanic rocks are generally lower than 5 mg/kg on average, but that volcanic glasses can contain higher levels, around 6 mg/kg on average (Smedley and Kinniburgh, 2002; Bundschuh et al., 2004). Boyle and Jonasson (1973) reported concentrations of 3.2–5.4 mg/kg of As in rhyolites, and other studies have found concentrations of 6–10 mg/kg of As in pyroclastic rocks containing over 90% of rhyolitic glass (Nicolli et al., 1989, 2010; Smedley et al., 1998).

In addition to total As concentrations in the rocks, the concentrations of the water-soluble fraction of As and other trace elements were measured in leachates extracted from
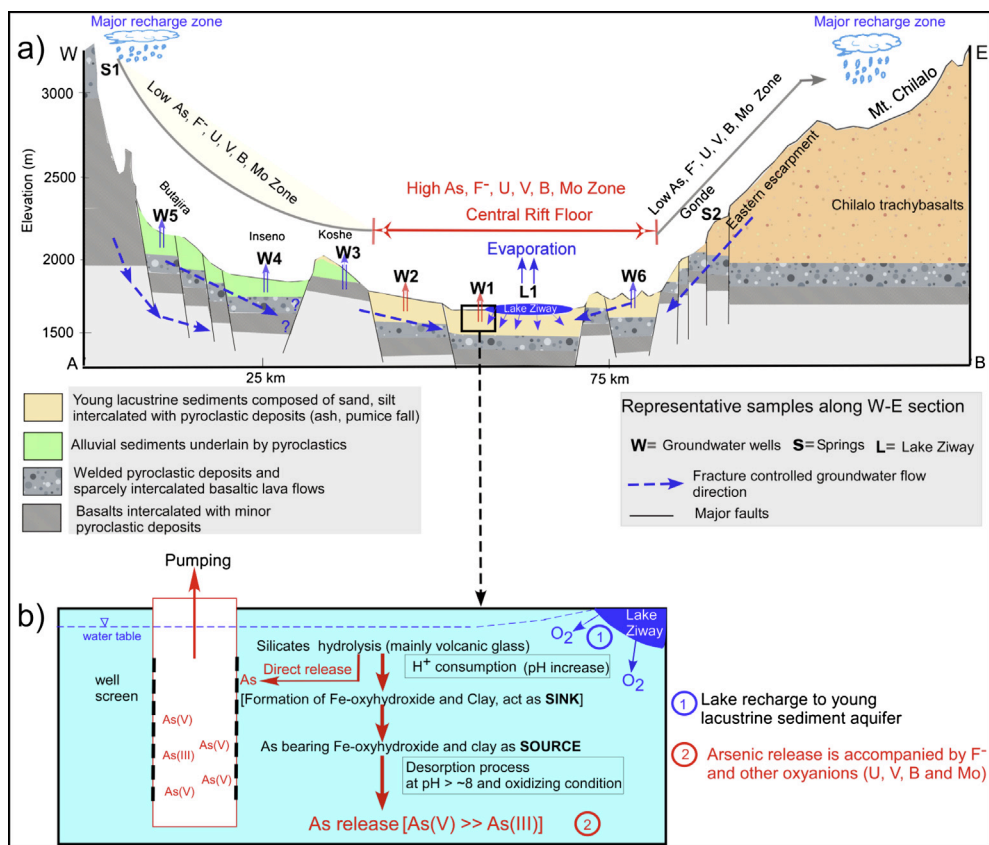

Fig. 4 – a) Simplified geological cross-section showing aquifer units and regional groundwater flow gradient along the Rift valley in Ziway-Shala basin, and indicating major zone of contamination by As and other toxic elements **b)** Proposed As release mechanism in the sedimentary aquifers west of Lake Ziway. As-bearing Fe-oxyhydroxides are postulated to be the dominant sink under oxidizing conditions and the dominant source under high pH conditions, Note: Summary of the average concentrations of major and trace elements in group of water samples at each W is displayed on Table 4. Lithological log of representative wells drilled in Zone W1 is showed in Fig. 5.
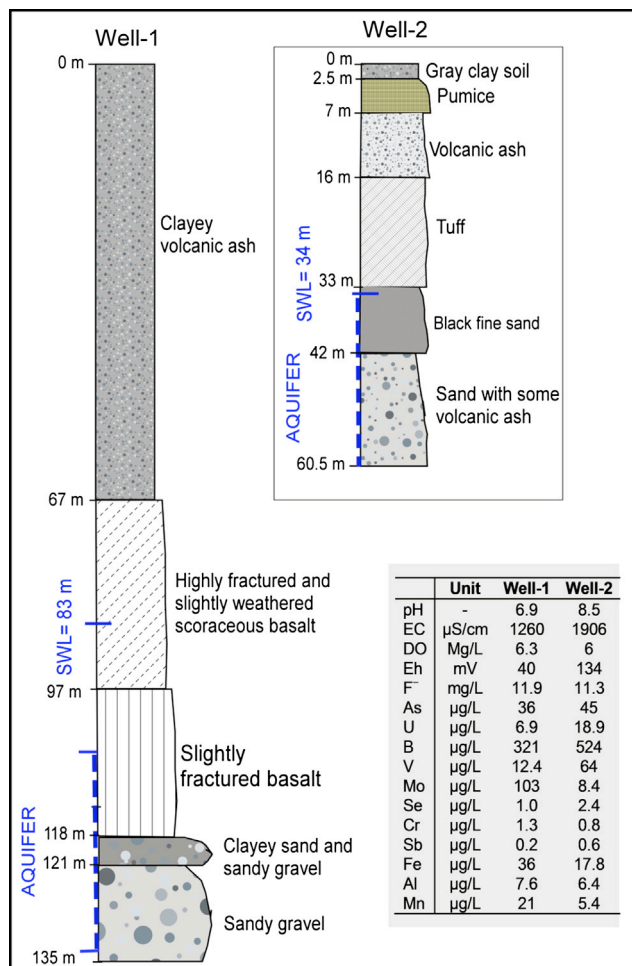
Fig. 5 — Lithological logs of representative boreholes drilled in lacustrine sediments at west of Lake Ziway (at W1; Fig. 4).

the sediments using double distilled water (Table 3c). The lacustrine sediments released the highest As concentrations (6.8, 3.5 and 1.5 mg/kg), whereas leachates from rhyolites samples released much lower As (<0.03 mg/kg). The average As in the lacustrine sediment leachates was 1.7 mg/kg, which is significantly (170 fold) higher than that found in the rock leachates (0.01 mg/kg). These analyses highlight the enrichment of As in the lake sediments, probably due to recycling through dissolution of rhyolitic glass and secondary co-mineralization during lake sediment deposition.

The apparent mismatch between the elevated As contents in MER groundwater and the aquifer rocks has reported previously in other cases; other studies have demonstrated the occurrence of high-As groundwater in unconsolidated sedimentary aquifers that do not contain exceptionally high As concentrations (e.g. Harvey et al., 2002; Smedley et al., 2005). We suggest that despite the low content of total As in the MER rocks and derived sediments, the elevated As concentration exceeding the drinking water threshold of 10 µg/L in MER groundwater is triggered by the specific hydrogeochemical conditions of the aquifers. In particular, the aquifers contain unconsolidated young pyroclastic materials that are highly reactive and generate high-pH, SiO_2-rich, and Na^+–HCO_3^- type groundwater. Considering that the dissolution of volcanic ash is the primary and dominant source of As and SiO_2, the concentrations of As, F^- and the other oxyanion-forming elements including U, B, V, and Mo, might also be expected to be distributed uniformly in MER groundwater, contrary to what was actually observed. We therefore suggest that secondary mineral phases, such as Fe-oxides and -oxyhydroxides, retain the bulk of the oxyanion-forming elements and their release from these minerals to the ambient groundwater depends on combined geochemical conditions, such as the groundwater pH that control the desorption of oxyanions from these mineralogical phases.
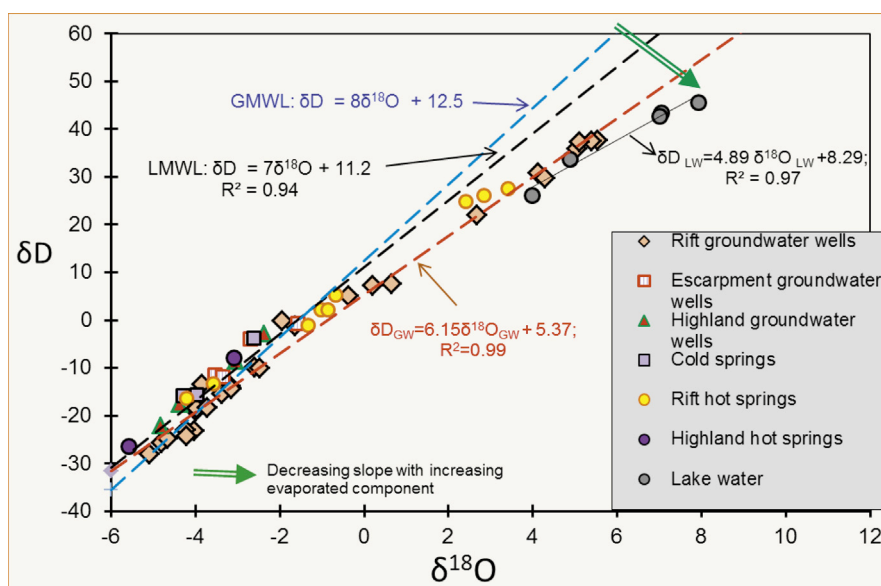

Fig. 6 — Isotopic compositions of MER groundwaters ($\delta D_{GW} = 6.15\delta^{18}O_{GW} + 5.37$; $R^2 = 0.99$, $n = 27$) are compared to the Local Meteoric Water Line (LMWL: $\delta D = 7\delta^{18}O + 11.2$; $R^2 = 0.94$, $n = 42$; Rango et al., 2010b), lakes ($\delta D_{GW} = 4.89\delta^{18}O_{LW} + 8.29$; $R^2 = 0.97$, $n = 5$). Note the decrease in the slope of linear regression lines indicating the increasing effect of evaporation on MER waters.

The most widely accepted mechanism for mobilizing As in oxidizing systems is desorption of As from hydrous metal oxides and clay minerals under high pH condition (Robertson, 1989; Welch et al., 2000; Smedley and Kinniburgh, 2002; Bhattacharya et al., 2006). Fe-oxides and -oxyhydroxides have the highest capacity and are the most important adsorbents of arsenates because of their strong binding affinity. Adsorption of arsenate is strongest at near-neutral pH, and decreases with pH, with minimum adsorption above pH ~8.5 (Masscheleyn et al., 1991; Goldberg and Johnston, 2001). Our data is consistent with this model; the MER groundwater had higher concentrations of As and other oxyanions in groundwater of pH >8. Groundwater with pH ranging between 8 and 8.9, for example contained average As concentrations of 33 µg/L, compared to 11 µg/L in waters with pH between 6.8 and 8. We conclude that the long-term flow of groundwater through the Rift Valley has generated weathered products that had

become a sink for oxyanion-forming elements. Continuous silicate hydrolysis (generating high-pH alkaline groundwater) induced the mobilization and release of oxyanion-forming elements. Fig. 4 illustrates the major aquifer units, groundwater evolution paths, and the proposed As and other oxyanion-forming elements release mechanisms in the MER sedimentary aquifers Fig. 5.

The positive relationship of As with F⁻ and the other oxyanion-forming elements suggests a common source for these elements. Similar relationships among these ions are found in aquifers containing volcanic ash and high-As concentrations in Argentina (Smedley et al., 2002; Bhattacharya et al., 2006). The co-occurrence of other oxyanion ions may also allow As to be mobilized from hydrous metal oxides into the groundwater, as a result of a competition for common adsorption sites. Jeong et al. (2007) have demonstrated As adsorption onto some oxides and clays in the presence of
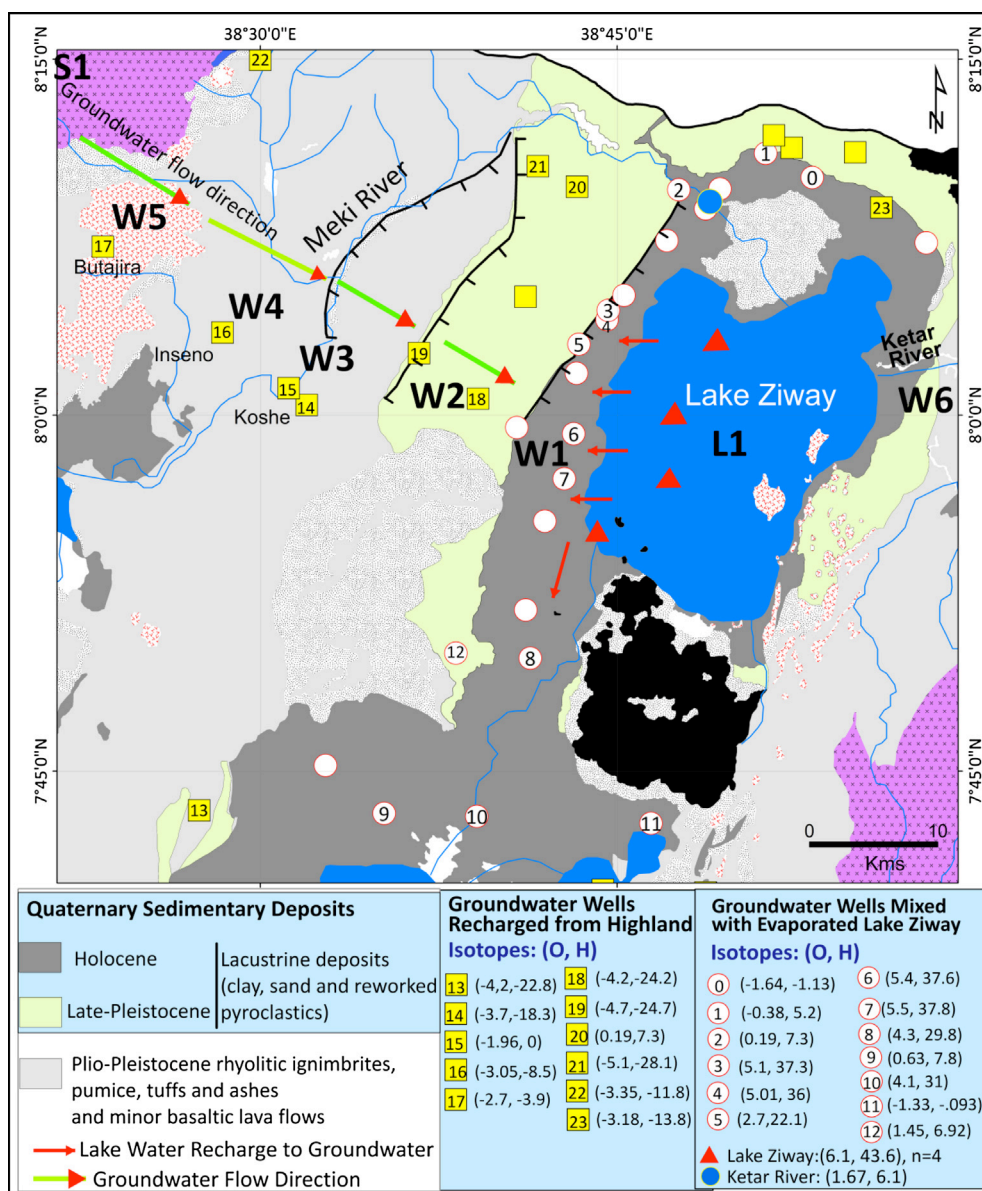

Fig. 7 – Spatial variation of stable isotopes along groundwater flow direction. Variation in concentrations of As, F⁻ and other trace elements at the area W1, W2, W3, W4, and W5 (see also Table 4).

Table 4 — Statistical summary (mean ± S.D) of major and selected trace elements concentrations in representative water samples taken from different aquifers located along the cross-section indicated in Fig. 4. SD-Standard Deviation.

Sampling area		Ziway		Koshe	Inseno	Butajira	Ogolcho	Lake Ziway	Acheber	Gonde
Zones (shown on Fig. 4)		W1 (n = 19)	W2 (n = 5)	W3 (n = 2)	W4 (n = 2)	W5 (n = 3)	W6 (n = 1)	L1 (n = 1)	S1 (n = 1)	S2 (n = 1)
Aquifer type		Lacustrine sediments		Fluvial sediments and fractured ignimbrite	Pyroclastic materials (ash, pumice)	Colluvial sediments	Fluvio-lacustrine sediments	—	Fractured basalt and ignimbrite	Fractured basalt and ignimbrite
pH	—	8.12 ± 0.5	7.84 ± 0.56	7.44 ± 0.23	7.33 ± 0.04	6.90 ± 0.06	7.57	9.06	6.84	6.95
EC	μS/cm	1859 ± 837	860 ± 312	792 ± 148	778 ± 135	433 ± 81.0	386	461	106	88
DO	mg/L	6.70 ± 1.9	7.85 ± 3.9	7.10 ± 4.38	9.30 ± 1.13	12.5 ± 2.20	7.30	11.1	10.6	19.5
Eh	mV	88.0 ± 60.1	75.6 ± 50.5	63.0 ± 33.0	81.0 ± 11.3	83.0 ± 55.0	69	55	133	166
Temp.	OC	27.6 ± 2.60	28.3 ± 4.8	30.0 ± 9.60	24.4 ± 1.13	22.0 ± 1.27	24.5	26.6	19.3	15.4
Na^+	mg/L	424 ± 233	182 ± 64.5	131 ± 43.0	118 ± 67	22.4 ± 3.15	66.4	82	12.0	4.01
Ca^{2+}	mg/L	13.9 ± 21.9	14.7 ± 7.15	36.0 ± 22.0	56.0 ± 12.7	55 ± 11.5	13.9	14.4	8.89	10.1
Mg^{2+}	mg/L	5.77 ± 8.81	2.69 ± 1.25	8.62 ± 6.58	14.6 ± 4.02	12.4 ± 2.73	2.90	8.63	2.16	3.31
NO_3^-	mg/L	0.80 ± 1.08	0.63 ± 0.6	0.82 ± 0.77	0.95 ± 0.61	0.92 ± 0.07	0.07	0.82	0.27	0.27
SO_4^{2-}	mg/L	50.0 ± 110	24.7 ± 26.8	8.48 ± 3.30	11.9 ± 4.6	5.56 ± 5.11	4.33	8.65	1.15	2.62
HCO_3^-	mg/L	968 ± 368	423 ± 78.9	454 ± 9.90	465 ± 140	239 ± 31.7	180	267	72	54
Cl^-	mg/L	79.7 ± 77.0	27 ± 20.6	10.0 ± 0.06	20.1 ± 1.7	10.4 ± 10	2.35	15.9	1.39	2.80
Br^-	mg/L	0.65 ± 0.42	0.24 ± 0.17	0.21 ± 0.06	0.23 ± 0.05	0.13 ± 0.04	0.05	0.17	0.05	0.05
SiO_2	mg/L	84.0 ± 8.90	90 ± 18.2	97.0 ± 20.0	87.0 ± 1.36	84 ± 2.15	87	37.5	57.4	46.6
TDS	mg/L	1556 ± 678	682 ± 180	652 ± 22.4	674 ± 168	340 ± 50	273	400	99	77
Field parameters and major ions										
F^-	mg/L	13.2 ± 14.0	6.60 ± 4.22	2.54 ± 0.63	2.23 ± 1.11	0.48 ± 0.05	3.48	1.81	0.47	0.20
As	μg/L	44.0 ± 46.0	18.9 ± 10.1	4.06 ± 0.52	1.62 ± 0.48	0.65 ± 0.18	0.58	2.39	0.34	0.25
U	μg/L	19.0 ± 19.5	5.80 ± 0.83	2.30 ± 0.65	13.1 ± 3.25	2.62 ± 2.67	0.42	1.40	0.07	0.11
B	μg/L	532 ± 465	169 ± 131	81.0 ± 7.13	10.0 ± 5.17	10.0 ± 5.12	19.12	87.3	4.81	3.56
Mo	μg/L	28.5 ± 39.0	51.0 ± 34.4	5.14 ± 3.28	2.34 ± 0.38	0.83 ± 0.29	9.89	4.30	0.70	0.33
V	μg/L	41.0 ± 36.5	45.6 ± 43.7	2.67 ± 0.48	21.6 ± 7.04	7.01 ± 0.21	2.76	9.71	11.4	6.62
Cr	μg/L	3.30 ± 3.65	0.69 ± 0.42	0.53 ± 0.02	1.75 ± 0.36	1.51 ± 1.03	0.36	2.45	0.66	2.08
Sb	μg/L	0.42 ± 0.32	0.09 ± 0.05	0.03 ± 0.03	0.06 ± 0.02	0.04 ± 0.04	0.02	0.17	0.00	0.00
Se	μg/L	3.58 ± 4.14	0.90 ± 0.37	1.15 ± 0.20	1.16 ± 0.74	0.99 ± 0.81	0.00	0.95	0.12	0.27
Fe	μg/L	48.0 ± 52.0	33.5 ± 16.0	85.0 ± 63.0	109 ± 5.53	137 ± 99.0	11.14	354	203	445
Mn	μg/L	38.0 ± 137	7.74 ± 9.33	334 ± 452	206 ± 286	21.8 ± 30.5	0.18	23.2	4.77	7.86
Al	μg/L	14.9 ± 28.4	7.5 ± 3.64	12.0 ± 9.60	6.47 ± 1.03	12.3 ± 5.95	1.81	1100	980	1996
Stable isotopes		W1 (n = 11)	W2 (n = 3)	W3 (n = 2)	W4 (n = 1)	W5 (n = 2)	W6 (n = 1)	L1 (n = 4)	S1 (n = 1)	S2 (n = 1)
$\delta^{18}O$	‰	2.72 ± 2.57	−4.7 ± 0.44	−2.85 ± 1.25	−3.05	−3.03 ± 0.45	−3.86	6.1 ± 0.93	−3.86	−3.18
δD	‰	22.2 ± 14.6	−25.7 ± 2.1	−9.16 ± 13	−8.52	−7.89 ± 5.61	−13.4	43.6 ± 7	−13.37	−13.8

elevated SiO_2, HCO_3^- and Se concentrations. The results of this study can be compared to other semi-arid and oxidizing aquifer systems that are also characterized by high As, including the Caco-Pampean plain and loess aquifers in Argentina (Nicolli et al., 1989; Bundschuh et al., 2004; Gomez et al., 2009), high plains of Texas, USA (Nativ and Smith, 1987; Gosselin et al., 2006; Scanlon et al., 2009), and in the Taiyuan basin of northern China (Guo et al., 2007). Collectively, these studies show a link between enrichment of As and other oxyanion complexes, including U, B, V, and Mo that is likely due to optimization of desorption and release from oxides and clay minerals to the ambient groundwater.

3.7. Water sources as detected by stable isotope in groundwater

Water sources in the MER system was evaluated based on oxygen and hydrogen isotopic variations. Groundwater wells ($n = 35$) had $\delta^{18}O$ ranging from -5% to $+5.5\%$ and δD ranging from -28% to $+37.8\%$, hot springs ($n = 9$) $\delta^{18}O$ between -4.2% and $+3.4\%$ and δD between -16.4 and $+27.6\%$; and lake samples ($n = 5$) ranged from $+3.98\%$ to $+7.92\%$ for $\delta^{18}O$ and from $+26.2\%$ to $+45.7$ for δD. This wide range in $\delta^{18}O$ and δD values reflect different water sources, evaporation, and mixing processes in the basin. The δD and $\delta^{18}O$ values in the MER groundwater lie along a line ($\delta D_{GW} = 6.15 \; \delta^{18}O_{GW} + 5.37$; $R^2 = 0.99$; $n = 27$) with a lower slope than the Local Meteoric Water Line (LMWL) (Fig. 6). The lower $\delta D/\delta^{18}O$ slope indicates groundwater recharge by some component of evaporated lake water (Fig. 6).

The spatial distribution of δD and $\delta^{18}O$ in groundwater west of Lake Ziway demonstrates two types of groundwater recharge (Fig. 7); groundwater from areas marked W2 to W5 was depleted in ^{18}O and δD and are consistent with low δD and $\delta^{18}O$ that characterizes the highland groundwater. This suggests that most of the groundwater in this area was originated from a lateral flow from the western escarpment of the Rift Valley. In contrast, groundwater from the Holocene sediments aquifer (W1 in Fig. 7) had much higher δD and $\delta^{18}O$ values that resemble the composition of the nearby Lake Ziway water with enriched ^{18}O and D ($\delta^{18}O = +6.1\%$, $\delta D = +43.6\%$; $n = 4$). Given the depth of the groundwater table ($18-97$ m) we

Fig. 8 – The association of As and $\delta^{18}O$ in MER groundwater.

exclude the possibility of evaporation of the groundwater, and therefore hypothesize that the Holocene aquifer (W1) is recharged by Lake Ziway surface water. Using a binary mixing model, wells in W1 aquifer (e.g. well #3, 4, 6 and 7; Fig. 7) seem to be originated from a blend of 90% from Lake Ziway water and 10% from western groundwater flow that characterizes W2 to W5 areas (Fig. 7).

The two different water sources are also associated with different contaminants levels. Groundwater from aquifers W2 to W5 had low salinity and low concentrations of trace elements relative to groundwater from the Holocene aquifer (W1) with elevated TDS 1556 ± 678 mg/L ($n = 19$) and high concentrations of As (44.4 μg/L), U (19 μg/L) and F⁻ (13.3 mg/L) (Table 4). Fig. 8 shows the relationship between As and $\delta^{18}O$ that suggests that the high As is linked to the enriched ^{18}O lake water. However, the high concentrations of contaminants in the Holocene aquifer could not be derived directly from the recharge of Lake Ziway given the relatively lower salinity (TDS = 400 mg/L) and lower concentrations of As (2.4 μg/L), U (1.4 μg/L), and F⁻ (1.8 mg/L) in Lake Ziway. Instead, we propose that the recharge of Lake Ziway water has triggered further mobilization of As and the other oxyanion-forming elements that led to their enrichment in groundwater of the Holocene aquifer. The distinct $\delta^{18}O$ and δD zones between the Holocene (W1) and the late Pleistocene aquifer (W2) may be explained by the presence of a large fault separating the two aquifers. The fault may act as a barrier by diverting the groundwater coming from the highland before it reaching to W1 (see Fig. 7). This can limit flushing and circulation of the groundwater in the Holocene aquifer and further explain the enrichment of contaminants in the aquifer.

The alkaline and high saline lakes in the Rift floor could also affect the adjacent groundwater. Lake Abijata for instance is highly affected by evaporation, as shown by the high enrichment of stable isotopes ($\delta^{18}O = +7.92$, $\delta D = +45.7$) and salinity (Cl = 5700 mg/L). However, the concentration of chloride in the groundwater north of the lake is not relatively high (95 mg/L; $n = 4$) to suggest a major recharge of the lake water to the regional groundwater in this area. This is consistent with groundwater flow simulations that have shown that groundwater flow from Abijata Lake is minimal (Ayenew, 2001). Lake Shala is also enriched in stable isotopes ($\delta^{18}O = +6.94$, $\delta D = +47.2$) and salinity (Cl = 3060 mg/L). High discharge hot springs (mean: 73 °C; $n = 3$) are located east of the lake with average $\delta^{18}O = +2.88$ and $\delta D = +26.3$, which suggests some contribution of the lake water to the hot spring.
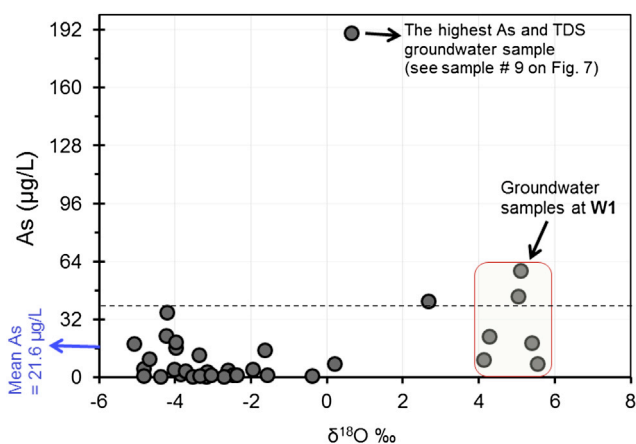
4. Conclusion

Elevated concentrations of As and other oxyanion-forming elements such as B, V, and Mo were found in groundwater from the main Ethiopian Rift Valley. The groundwater is characterized by high mineralization (TDS up to 3560 mg/L), high pH (6.8–8.9), predominance of Na^+ and HCO_3^-, positive Eh, high concentrations of dissolved O_2, and low Fe and Mn concentrations. In most groundwater, As is composed of mainly (80%) arsenate-As(V) species rather than arsenite-

As(III). A small subset of groundwater samples were found to be under reducing conditions with high levels of Fe and Mn, and low levels of U and V. A model was developed to explain the enrichment mechanism of As and the other oxyanion-forming elements in the MER Quaternary sedimentary aquifers. The unconfined aquifers are predominantly constituted of sandy and silty pyroclastic materials, rich in volcanic glass (on average >65 wt% SiO_2). Total As contents in rhyolites and lake sediments aquifer materials were found to be in a range of 1.1–3.5 mg/kg (mean: 2.5 mg/kg) and 1.4–16.1 mg/kg (mean: 6.6 mg/kg), respectively. The highest As concentrations (16.1 mg/kg) were found in the lacustrine sediments relative to the rhyolitic rocks (mean 3.5 mg/kg). The lacustrine sediments also contained on average 3.5 mg/kg of U, 62 mg/kg of V, 136 mg/kg of Mo and 6.7 mg/kg of Cr. We propose that the weathering of volcanic materials has produced weathering products such as iron oxides and clay minerals, which act as sinks for As and other oxyanion-forming elements. The current high level of As in the groundwater is primarily due to desorption from Fe-oxide and -oxyhydroxide minerals under alkaline pH >∼8 and oxidative conditions. The elevated groundwater pH is therefore one of the most significant factors controlling the mobility of As and the other oxyanion-forming elements. The use of stable isotopes enable us to delineate zone of different water sources in the Ziway-Shala basin, in particular to distinguish recharge water from lateral and regional flow from the Rift escarpment and local recharge water of Lake Ziway to the adjacent aquifer. Our finding show that groundwater from the local aquifer, west of Lake Ziway, is highly enriched in As and other oxyanion-forming elements and thus pose a significant health risk to the local population. This study represents an important case study of As and other oxyanion-forming elements occurrences in oxidizing aquifers of the semi-arid basins in the MER, which is similar in geology and climate to other neighbouring regions of the East African Rift System.

Author contributions

T.R., and A.V., designed research.
 T.R., and A.V., performed research.
 T.R., and A.V., analyzed data.
 T.R., and A.V., wrote the paper; and.
 G.D., G.B., and T.R., contributed in analytical tools.

Funding sources

Disclaimer

The findings and conclusions in this report are those of the authors and do not necessarily represent the official position of the funding sources.

Conflict of interest

The authors declare they have no actual or potential competing financial interests.

Acknowledgements

REFERENCES

Ayenew, T., 1998. The Hydrogeological System of the Lake District Basin, Central Main Ethiopian Rift. Free University of Amsterdam, The Netherlands. PhD Thesis.

Ayenew, T., 2001. Numerical groundwater flow modeling of the Central Main Ethiopian Rift lakes basin. SINET: Ethiopian Journal of Science 24 (2), 167–184.

Ayenew, T., Kebede, S., Alemyahu, T., 2007. Environmental isotopes and hydrochemical study as applied to surface water and groundwater interaction in the Awash river basin. Hydrological Processes 8. http://dx.doi.org/10.1007/s00254-007-0914-4. Published online.

Ayenew, T., Demlie, M., Wohnlich, S., 2008. Hydrogeological framework and occurrence of groundwater in the Ethiopian aquifers. Journal of African Earth Sciences 52, 97–113.

Benvenuti, M., Carnicelli, S., Belluomini, G., Dainelli, N., Di Grazia, S., Ferrari, G.A., Iasio, C., Sagri, M., Ventra, D., Atnafu, B., Kebede, S., 2002. The Ziway–Shala basin (Main Ethiopian rift, Ethiopia): a revision of basin evolution with special reference to the late quaternary. Journal of African Earth Sciences 35, 247–269.

Bhattacharya, P., Chatterjee, D., Jacks, G., 1997. Occurrence of arsenic-contaminated groundwater in alluvial aquifers from delta plains, eastern India: options for safe drinking water supply. International Journal of Water Resources Development 13, 79–92.

Bhattacharya, P., Jacks, G., Ahmed, K.M., Khan, A.A., Routh, J., 2002. Arsenic in groundwater of the Bengal Delta Plain aquifers in Bangladesh. Bulletin of Environmental Contamination and Toxicology 69, 538–545.

Bhattacharya, P., Claesson, M., Bundschuh, J., Sracek, O., Fagerberg, J., Jacks, G., Martin, R.A., Storniolo, A.D., Thir, J.M., 2006. Distribution and mobility of arsenic in the Rio Dulce alluvial aquifers in Santiago del Estero Province, Argentina. Science of the Total Environment 358, 97–120.

Borgono, J.M., Vicent, P., Venturino, H., Infante, A., 1977. Arsenic in the drinking water of the city of Antofagasta: epidemiological and clinical study before and after the installation of the treatment plant. Environmental Health Perspectives 19, 103–105.

Boyle, R.W., Jonasson, I.R., 1973. The geochemistry of as and its use as an indicator element in geochemical prospecting. Journal of Geochemical Exploration 2, 251–296.

Bretzler, A., Osenbrück, K., Gloaguen, R., Ruprecht, J.S., Kebede, S., Stadler, S., 2011. Groundwater origin and flow dynamics in active rift systems – a multi-isotope approach in the Main Ethiopian Rift. Journal of Hydrology 402, 274–289.

Bundschuh, J., Farias, B., Martin, R., Storniolo, A., Bhattacharya, P., Cortes, J., Bonorino, G., Albouy, R., 2004. Groundwater arsenic in the Caco-Pampean plain, Argentina: case study from Robles county Santiago del Estero Province. Applied Geochemistry 19, 231–243.

Chakraborti, D., Rharman, M.M., Paul, K., Chowdhury, U.K., Sengupta, M.K., Lodh, D., Chanda, C.R., Saha, K.C., Mukherjee, S.C., 2002. Arsenic calamity in the Indian subcontient. What lessons have been learned? Talanta 58, 3–22.

Cheng, T.J., Ke, D.S., Guo, H.-R., 2010. The association between arsenic exposure from drinking water and cerebrovascular disease mortality in Taiwan. Water Research 44, 5770–5776.

Chernet, T., Travi, Y., Valles, V., 2001. Mechanism of degradation of the quality of natural water in the lakes region of the Ethiopian Rift Valley. Water Research 35, 2819–2832.

Clark, I.D., Fritz, P., 1997. Environmental Isotopes in Hydrogeology. CRC Press/Lewis Publishers, Boca Raton, FL, p. 328.

Darling, G., Gizaw, B., Arusei, M., 1996. Lake–groundwater relationships and fluid–rock interaction in the East African Rift Valley: isotopic evidence. Journal of African Earth Sciences 22, 423–430.

Das, D., Chatterjee, A., Samanta, G., Mandal, B.K., Chowdhury, T.R., Chowdhury, P.P., Chanda, C., Basu, G., Lodh, D., Nandi, S., Chakraborty, T., Mandal, S., Bhattacharya, S.M., Chakraborti, D., 1994. Arsenic in groundwater in six districts of West Bengal, India: the biggest arsenic calamity in the world. Analyst 119, 168N–170N.

Dowling, C.B., Poreda, R.J., Basu, A.R., Peters, S.L., Aggarwal, P.K., 2002. Geochemical study of arsenic release mechanisms in the Bengal Basin groundwater. Water Resources Research 38, 1173. http://dx.doi.org/10.1029/2001/WR000968.

Elinder, C.G., 1986. Zinc. In: Friberg, L., Nordberg, G.F., Vouk, V.B. (Eds.), Handbook on the Toxicology of Metals, second ed. Elsevier Science Publishers, Amsterdam, pp. 664–679.

Ethiopian Mapping Authority, 1988. National Atlas of Ethiopia. Ethiopian Mapping Authority, Addis Ababa, Ethiopia.

Furi, W., Razack, M., Haile, T., Abiye, T.A., Ayenew, T., Legesse, D., 2011. Fluoride enrichment mechanism and geospatial distribution in the volcanic aquifers of the Middle Awash basin. Northern Main Ethiopian Rift Journal of African Earth Science 60, 315–327.

Gizaw, B., 1996. The origin of high bicarbonate and fluoride concentrations in waters of the Main Ethiopian Rift Valley, East African Rift System. Journal of African Earth Sciences 22 (4), 391–402.

Goldberg, S., Johnston, C.T., 2001. Mechanisms of arsenic adsorption on amorphous oxides evaluated using macroscopic measurements, vibrational spectroscopy, and surface complexation modeling. Journal of Colloid and Interface Science 234, 204–216.

Gomez, M.L., Blarasin, M.T., Martinez, D.E., 2009. Arsenic and fluoride in a loess aquifer in the central area of Argentina. Environmental Geology 57, 143–155.

Gosselin, D.C., Klawer, L.M., Joeckel, R.M., Harvey, F.E., Reade, A.R., McVey, K., 2006. Arsenic in groundwater and rural public water supplies in Nebraska, USA. Great Plains Research 16, 137–148.

Guo, Q., Wang, Y., Gao, X., Ma, T., 2007. A new model (DRARCH) for assessing groundwater vulnerability to arsenic contamination at basin scale: a case study in Taiyuan basin, northern China. Environmental Geology 52, 923–932.

Harvey, C.F., Swartz, C.H., Badruzzaman, A.B.M., Keon-Blute, N., Yu, W., Ali, M.A., Jay, J., Beckie, R., Niedan, V., Brabander, D., Oates, P.M., Ashfaque, K.N., Islam, S., Hemond, H.F., Ahmed, M.F., 2002. Arsenic mobility and groundwater extraction in Bangladesh. Science 298, 1602–1606.

Jeong, Y., Maohong, F., Van Leeuwen, J., Belczyk, J.F., 2007. Effect of competing solutes on arsenic(V) adsorption using iron and aluminum oxides. Journal of Environmental Sciences 19, 910–919.

Kar, S., Maity, J.P., Jean, J.-S., Liu, C.-C., Nath, B., Yang, H.-J., Bundschuh, J., 2010. Arsenic-enriched aquifers: occurrences and mobilization of arsenic in groundwater of Ganges Delta Plain, Barasat, West Bengal, India. Applied Geochemistry 25, 1805–1814.

Kar, S., Maity, J.P., Jean, J.-S., Liu, C.-C., Nath, B., Lee, Y.-C., Bundschuh, J., Chen, C.-C., Li, Z., 2011. Role of organic matter and humic substances in the binding and mobility of arsenic in a Gangetic aquifer. Journal of Environmental Science and Health, Part A 46, 1231–1238.

Kloos, H., Tekle-Haimanot, R., 1999. Distribution of fluoride and fluorosis in Ethiopia and prospects for control. Tropical Medicine & International Health 4, 355–364.

Le Turdu, C., Tiercelin, J.J., Gibert, E., Travi, Y., Lezzar, K.E., Richert, J.P., et al., 1999. The Ziway–Shala lake basin system, Main Ethiopian Rift: influence of volcanism, tectonics, and climatic forcing on basin formation and sedimentation. Palaeogeography Palaeoclimatology Palaeoecology 150, 135–177.

Li, Z., Hong, H., Jean, J.-S., Koski, A.J., Liu, C.-C., Reza, S., Randolph, J.J., Kurdas, S.R., Friend, J.H., Antinucci, S.J., 2011. Characterization on arsenic sorption and mobility of the sediments of Chia-Nan plain, where black foot disease occurred. Environmental Earth Sciences 64, 823–831.

Lianfang, W., Jianzhong, H., 1994. Chronic arsenicism from drinking water in some areas of Xinjiang, China. In: Nriagu, J.O. (Ed.), Arsenic in the Environment, Part II: Human Health and Ecosystem Effects. John Wiley Inc, New York, pp. 159–172.

Liu, C.W., Wang, S.W., Jang, C.S., Lin, K.H., 2006. Occurrence of arsenic in ground water in the Choushui river alluvial fan, Taiwan. Journal of Environmental Quality 35, 68–75.

Lu, K.L., Liu, C.W., Wang, S.W., Jang, C.S., Lin, K.H., Liao, V.H.C., Liao, C.M., Chang, F.J., 2011. Assessing the characteristics of groundwater quality of arsenic contaminated aquifers in the blackfoot disease endemic area. Journal of Hazardous Materials 185, 1458–1466.

Masscheleyn, P.H., Delaune, R.D., Patrick, W.H., 1991. Effect of redox potential and pH on arsenic speciation and solubility in a contaminated soil. Environmental Science & Technology 25, 1414–1419.

Meurer, W.P., Wilmore, C.C., Boudreau, A.E., 1999. Metal redistribution during fluid exsolution and migration in the middle Banded series of the Stillwater Complex, Montana. Lithos 47, 143–156.

Mukherjee, A.B., Bhattacharya, P., 2001. Arsenic in groundwater in the Bengal Delta Plain: slow poisoning in Bangladesh. Environmental Reviews 9, 189–220.

Mukherjee, A., von Brömssen, M., Scanlon, B.R., Bhattacharya, P., Fryar, A.E., Hasan, Md.A., Ahmed, K.M., Chatterjee, D., Jacks, G., Sracek, O., 2008. Hydrogeochemical comparison and effects of overlapping redox zones on groundwater arsenic near the Western (Bhagirathi sub-basin, India) and Eastern (Meghna sub-basin, Bangladesh) margins of the Bengal Basin. Journal of Contaminant Hydrology 99, 31−48.

Nath, B., Stüben, D., Basu Mallik, S., Chatterjee, D., Charlet, L., 2008a. Mobility of arsenic in West Bengal aquifers conducting low and high groundwater arsenic, Part I: comparative hydrochemical and hydrogeological characteristics. Applied Geochemistry 23, 977−995.

Nath, B., Jean, J.-S., Lee, M.-K., Yang, H.-J., Liu, C.-C., 2008b. Geochemistry of high arsenic groundwater in Chia-Nan plain, Southwestern Taiwan: Possible sources and reactive transport of arsenic. Journal of Contaminant Hydrology 99, 85−96.

Nath, B., Maity, J.P., Jean, J.-S., Birch, G., Kar, S., Yang, H.-J., Lee, M.-K., Hazra, R., Chatterjee, D., 2011. Geochemical characterization of the arsenic-affected alluvial aquifers of the Bengal Delta (West Bengal and Bangladesh) and Chianan Plains (SW Taiwan): implications for human health. Applied Geochemistry 26, 705−713.

Nativ, R., Smith, D.A., 1987. Hydrogeology and geochemistry of the Ogallala aquifer, southern high plains. Journal of Hydrology 91, 217−253.

Nickson, R.T., McArthur, J.M., Ravenscroft, P., Burgess, W.G., Ahmed, K.M., 2000. Mechanism of arsenic release to groundwater, Bangladesh and West Bengal. Applied Geochemistry 15, 403−413.

Nicolli, H.B., Suriano, J.M., Gomez Peral, M.A., Ferpozzi, L.H., Baleani, O.A., 1989. Groundwater contamination with arsenic and other trace elements in an area of the Pampa, Province of Córdoba, Argentina. Environmental Geology and Water Sciences 14, 3−16.

Nicolli, H.B., Bundschuh, J., García, J.W., Falcón, C.M., Jean J-, S., 2010. Sources and controls for the mobility of arsenic in oxidizing groundwaters from loess-type sediments in arid/semi-arid dry climates—evidence from the Chaco−Pampean plain (Argentina). Water Research 44, 5589−5604.

Di Paola, G.M., 1972. The Ethiopian rift valley (between 7 000 and 8 400 lat. North). Bulletin of Volcanology 36, 517−560.

Parkhurst, D.L., Appelo, C.A.J., 1999. Users Guide to PHREEQC (Version 2): a Computer Program for Speciation, Batch-reaction, One-dimensional Transport, and Inverse Geochemical Modeling, pp. 99−4259. US Geological Survey Water Resources Investigation Report.

Peccerillo, A., Donati, C., Santo, A.P., Orlando, A., Yirgu, G., Ayalew, D., 2007. Petrogenesis of silicic peralkaline rocks in the Ethiopian Rift: geochemical evidence and volcanological implications. Journal of African Earth Sciences 48, 161−173.

Rango, T., Bianchini, G., Beccaluva, L., Ayenew, T., Colombani, N., 2009. Hydrogeochemical study in the main Ethiopian Rift: new insights to source and enrichment mechanism of fluoride. Environmental Geology 58, 109−118.

Rango, T., Bianchini, G., Beccaluva, L., Tassinari, R., 2010a. Geochemistry and water quality assessment of central main Ethiopian Rift natural waters with emphasis on source and occurrence of fluoride and arsenic. Journal of African Earth Sciences 57, 479−491.

Rango, T., Petrini, R., Stenni, B., Bianchini, G., Slejko, F., Beccaluva, L., Ayenew, T., 2010b. The dynamics of central main Ethiopian Rift waters: evidence from δD, $\delta^{18}O$ and $^{87}Sr/^{86}Sr$ ratios. Applied Geochemistry 25, 1860−1871.

Rango, T., Kravchenko, J., Atlaw, B., Peter, G.M., Jeuland, M., Merola, B., Vengosh, A., 2012. Groundwater quality and its health impact: an assessment of dental fluorosis in rural inhabitants of the main Ethiopian Rift. Environment International 43, 37−47.

Reimann, C., Bjorvatn, K., Frengstad, B., Melaku, Z., Tekle-Haimanot, R., Siewers, U., 2003. Drinking water quality in the Ethiopian section of the East African Rift Valley I−data and health aspects. The Science of the Total Environment 311 (1−3), 65−80.

Reza, A.H.M.S., Jean, J.-S., Yang, H.-J., Lee, M.-K., Yang, H.-J., Liu, C.-C., 2010. Arsenic enrichment and mobilization in the Holocene alluvial aquifers of the Chapai-Nawabganj district, Bangladesh. Applied Geochemistry 25, 1280−1289.

Reza, A.H.M.S., Jean, J-h, Lee, M.-K., Kulp, T.R., Hsu, H.-F., Liu, C.-C., Lee, Y.-C., 2012. The binding nature of humic substances with arsenic in alluvial aquifers of Chianan Plain, southwestern Taiwan. Journal of Geochemical Exploration 114, 98−108.

Robertson, F.N., 1989. Arsenic in ground-water under oxidizing conditions, south-west United States. Environmental Geochemistry and Health 11, 171−185.

Sancha, A.M., O'Ryan, R., 2008. Managing hazardous pollutants in Chile: arsenic. Reviews of Environmental Contamination and Toxicology 196, 123−146.

Scanlon, B.R., Nicot, J.P., Reedy, R.C., Kurtzman, D., Mukherjee, A., Nordstrom, D.K., 2009. Elevated naturally occurring arsenic in a semiarid oxidizing system, Southern High Plains aquifer, Texas, USA. Applied Geochemistry 24, 2061−2071.

Smedley, P.L., Kinniburgh, D.G., 2002. A review of the source, behavior and distribution of arsenic in natural waters. Applied Geochemistry 17, 517−568.

Smedley, P.L., Nicolli, H., Barros, J., Tullio, O., 1998. Origin and mobility of arsenic in groundwater from the Pampean Plain, Argentina. In: 9th International Symposium Water−rock Interactions. Taupo, New Zealand.

Smedley, P.L., Nicolli, H.B., Macdonald, D.M.J., Barros, A.J., Tullio, J.O., 2002. Hydrochemistry of arsenic and other inorganic constituents in groundwater from La Pampa, Argentina. Applied Geochemistry 2002 (17), 259−284.

Smedley, P.L., Zhang, M.-Y., Zhang, G.-Y., Luo, Z.-D., 2003. Mobilisation of arsenic and other trace elements in fluviolacustrine aquifers of the Huhhot Basin, Inner Mongolia. Applied Geochemistry 18, 1453−1477.

Smedley, P.L., Kinniburgh, D.G., Macdonald, D.J.M., Nicolli, H.B., Barros, A.J., Tullio, J.O., Alonso, M.S., 2005. Arsenic associations in sediments from the loess aquifer of La Pampa, Argentina. Applied Geochemistry 20 (5), 989−1016.

Stumm, W., Morgan, J.J., 1996. Aquatic Chemistry: Chemical Equilibria and Rates in Natural Waters. Wiley-Interscience, New York.

Tekle-Haimanot, R., Fekadu, A., Bushra, B., 1987. Endemic fluorosis in the Ethiopian rift valley. Tropical and Geographical Medicine 39, 209−217.

Webster, J.G., 1999. Arsenic. In: Marshall, C.P., Fairbridge, R.W. (Eds.), Encyclopaedia of Geochemistry. Chapman Hall, London, pp. 21−22.

Welch, A.H., Lico, M.S., 1998. Factors controlling As and U in shallow groundwater, southern Carson Desert, Nevada. Applied Geochemistry 13, 521−539.

Welch, A.H., Westjohn, D.B., Helsel, D.R., Wanty, R.B., 2000. Arsenic in ground water of the United States: occurrence and geochemistry. Ground Water 38, 589−604.

WoldeGabriel, G., Aronson, J.L., Walter, R.C., 1990. Geology, geochronology, and Rift basin development in the central sector of the main Ethiopian Rift. Geological Society of America Bulletin 102, 439−458.

World Health Organisation, 2001. Environmental Health Criteria 224: Arsenic Compounds, second ed. WHO, Geneva.

Yirgu, G., Dereje, A., Peccerillo, A., Barberio, M.R., Donati, C., Donato, P., 1999. Fluorine and chlorine distribution in the volcanic rocks from the Gedemsa volcano, Ethiopian Rift Valley. Acta Vulcanologica 11, 169−176.

Yunus, M., Sohel, N., Hore, S.K., Rahman, M., 2011. Arsenic exposure and adverse health effects: a review of recent findings from arsenic and health studies in Matlab, Bangladesh. Kaohsiung Journal of Medical Sciences 27, 371—376.

Zheng, Y., Stute, M., van Geen, A., Gavriela, I., Dhar, R., Simpson, H., Schlosser, P., Ahmed, K.M., 2004. Redox control of arsenic mobilization in Bangladesh groundwater. Applied Geochemistry 19, 201—214.